Supporting Information:

Accessing Multiple Catalytically Active States in Redox Controlled Olefin Polymerization

Minhui Zhao, Changle Chen[*]

CAS Key Laboratory of Soft Matter Chemistry, Department of Polymer Science and Engineering, University of Science and Technology of China, Hefei, 230026, China

changle@ustc.edu.cn

Table of Contents

1. Methods

General methods.

All experiments were carried out under a dry Nitrogen atmosphere using standard Schlenk techniques or in a glove-box. Deuterated solvents used for NMR were dried and distilled prior to use. ^{1}H, ^{13}C NMR spectra were recorded by a Bruker Ascend Tm 400 spectrometer at ambient temperature unless otherwise stated. The chemical shifts of the ^{1}H and ^{13}C NMR spectra were referenced to the residual solvent; Coupling constants are in Hz. ^{13}C NMR spectra of the polyethylene samples were obtained on 10-20 wt % solutions of the polymers and 0.05 M CrAcAc in 1,2,4-trichlorobenzene (TCB) unlocked at 120-140 ℃ using a 90° pulse of 17.8 μs, a spectral width of 35 kHz, a relaxation delay of 5 s, an acquisition time of 0.64 s, and inverse gated decoupling. Samples were preheated for at least 15 min before acquiring data. Elemental analysis was performed by the Analytical Center of the University of Science and Technology of China. MALDI MS was recorded on a Bruker Autoflex III smart beam instrument, using trans-2-[3-(4-tert-butylphenyl)-2-methyl-2- propenylidene] malononitrile (DCTB) as the matrix. FT-IR spectra were performed on a Bruker VECTOR-22 IR spectrometer. The spectra of all samples were collected at 64 scans with a spectral resolution of 4 cm^{-1} by the KBr disk method. X-ray Diffraction data were collected at 298(2) K on a Bruker Smart CCD area detector with graphite-monochromated Mo K^{α} radiation (λ = 0.71073 Å). The relative number-average molar masses (M_n, RI), the absolute weight-average molar masses M_w, MALLS) were determined at 35 ℃ by gel permeation chromatography (GPC, Waters 1515) equipped with three Waters Styragel columns (guard, HR 0.5, HR 1, and HR 4), a Waters 717 PLUS autosampler, a Waters 2414 differential refractometer, a multiangle-laser-light-scattering (MALLS) detector. The DRI increment dn/dc value of 0.078 mL/g was used for all polyethylene samples synthesized. Tetrahydrofuran (THF) was used as the eluent at a flow rate of 1.0 mL/min. 2,6-diisopropyl-4-ferroceneaniline[1], AgBAF[2] were prepared according to published procedures. All other reagents were purchased from commercial sources and used without purification.

Procedure for the Synthesis of Ligands.

(2,6-$^{i}Pr_2$-4-Fc-C_6H_2)N=C(CH_3)-(CH_3)C=N(2,6-$^{i}Pr_2$-4-Fc-C_6H_2) (**L-Fc**). A 50 mL round bottom flask was charged with 2,6-diisopropyl-4-ferroceneaniline (0.5 g, 1.39 mmol), 2,3-butanedione (0.06 g, 0.70 mmol), toluene (20 mL) and a catalytic amount of p-toluenesulfonic acid. After refluxing for 48h, the reaction mixture was cooled to room temperature and extracted with ethyl acetate, washed with brine, and dried over $MgSO_4$. The volatile fraction was evaporated and the residue was subjected to column chromatography (silica gel, petroleum ether/EtOAc (40:1)) to afford **L-Fc** as an orange solid (0.37 g, 66 %). ^{1}H NMR ($CDCl_3$, 400 MHz): δ 7.29(s, 4H, ArH), 4.62(s, 4H, C_5H_4), 4.28(s, 4H, C_5H_4), 4.06(s, 10H, C_5H_5), 2.74(sept, J = 6.8, 4H, C*H*Me_2), 2.11(s, 6H, N=C*Me*), 1.24(d, 24H, CH*Me*$_2$). ^{13}C NMR (101 MHz, $CDCl_3$) δ 168.68(N=*C*Me), 144.68, 135.16, 134.28, 121.60, 87.54, 69.73(*C*$_5$H$_4$), 68.61(*C*$_5$H$_4$), 66.77(*C*$_5$H$_4$), 28.72(*C*H(CH_3)$_2$), 23.35 (CH(*C*H_3)$_2$), 23.09(CH(*C*H_3)$_2$), 16.95(N=C*Me*). MALDI-TOF (m/z): calcd for C48H56Fe2N2, 772.3142; found: 772.2524. Anal. Calcd for $C_{48}H_{56}Fe_2N_2$: C, 74.61; H, 7.31; N, 3.63; Found: C, 74.98; H, 7.34; N, 3.61.

Procedure for the Synthesis of Palladium Complex.
[(2,6-$^{i}Pr_2$-4-Fc-C_6H_2)N=C(CH_3)-(CH_3)C=N(2,6-$^{i}Pr_2$-4-Fc-C_6H_2)]PdMeCl (**Pd-Cl**). A mixture of the ligand **L-Fc** (772 mg, 1 mmol), Pd(COD)MeCl (265 mg, 1 mmol) in CH_2Cl_2 (20 mL) was stirred for 12 h at room temperature. During stirring, the solid was completely dissolved and the color of the solution was changed from orange to dark red. At the end of the reaction, the desired compound was isolated using column chromatography. The mixture was eluted on silica gel with first 1:1 hexanes/CH_2Cl_2, then pure CH_2Cl_2 as the mobile phase. The pure compound was obtained as a red solid (874 mg, 94 %) . ^{1}H NMR ($CDCl_3$, 400 MHz): δ 7.33(d, J = 15.7 Hz, 4H, ArH), 4.63(d, J = 9.3 Hz, 4H, C_5H_4), 4.31(d, J = 17.2 Hz, 4H, C_5H_4), 4.07(d, J = 5.1 Hz 10H, C_5H_5), 3.07(sept, J = 6.6, 4H, C*H*Me_2), 2.07(d, J = 8.7 Hz, 6H, N=C*Me*), 1.44(dd, J = 30.8, 6.6 Hz, 12H, CH*Me*$_2$), 1.21(d, J = 6.7 Hz, 12H, CH*Me*$_2$), 0.58(s, 3H, Pd-C*H*$_3$). ^{13}C NMR (101 MHz, $CDCl_3$) δ 174.07(N=*C*Me), 169.39(N=*C*Me), 140.17, 139.97, 138.68, 138.39, 137.71, 137.54, 121.89, 121.55, 86.55(*C*$_5H_4$), 85.52(*C*$_5H_4$), 69.69(*C*$_5H_4$), 69.67(*C*$_5H_4$) (*C*$_5H_4$), 69.02(*C*$_5H_4$), 68.62(*C*$_5H_4$), 66.92(*C*$_5H_4$), 66.84(*C*$_5H_4$), 28.98(*C*H(CH_3)$_2$), 28.45(*C*H(CH_3)$_2$), 23.90(CH(*C*H_3)$_2$), 23.55(CH(*C*H_3)$_2$), 23.34(CH(*C*H_3)$_2$), 21.22(N=C*Me*), 19.83(N=C*Me*), 2.75(Pd-*C*H_3). MALDI-TOF (m/z): calcd for C49H59ClFe2N2Pd, 928.2100; found: 928.2465. Anal. Calcd for $C_{49}H_{59}ClFe_2N_2Pd$: C, 63.31; H, 6.40; N, 3.01; Found: C, 63.10; H, 6.43; N, 3.02.

Procedure for the Synthesis of Cationic Palladium Complex. {[(2,6-$^{i}Pr_2$-4-Fc-C_6H_2)N=C(CH_3)-(CH_3)C=N(2,6-$^{i}Pr_2$-4-Fc-C_6H_2)]PdMe(CH_3CN)}[BAF] **(Pd-CN).** A Schlenk flask was charged with NaBAF (886 mg, 1.0 mmol) and **Pd-Cl** (928 mg, 1.0 mmol) under a nitrogen atmosphere. Acetonitrile (15mL) was added to form a bright maroon solution, which was stirred overnight. The solution was filtered twice leaving behind a white precipitate of NaCl. The solid salt was rinsed twice with hexane. The solution was evaporated and the dark foam was dried overnight, affording 902 mg dark red powder (96%). ^{1}H NMR (400 MHz, CD_2Cl_2) δ 7.64 (s, 8H, Ar'H$_o$), 7.48 (s, 4H, Ar'H$_p$), 7.32 (s, 2H, ArH), 7.22 (s, 2H, ArH), 4.73 (d, J = 51.6 Hz, 4H, C_5H_4), 4.41 (d, J = 41.0 Hz, 4H, C_5H_4), 4.07 (d, J = 35.9 Hz, 8H, C_5H_4), 2.88 – 2.70 (m, 4H, C*H*Me_2), 2.17 (d, J = 2.2 Hz, 6H, N=C*Me*), 1.78 (s, 3H, NC*Me*), 1.33 (d, J = 6.8 Hz, 6H, CH*Me*$_2$), 1.28 (d, J = 6.8 Hz, 6H, CH*Me*$_2$), 1.21 (d, J = 6.9 Hz, 6H, CH*Me*$_2$), 1.15 (d, J = 6.8 Hz, 6H, CH*Me*$_2$), 0.49 (s, 3H, Pd-C*H*$_3$). ^{13}C NMR (101 MHz, CD_2Cl_2) δ 179.03(N=*C*Me), 171.52(N=CMe), 161.73, 161.24, 160.74, 160.25, 137.22, 136.77, 134.04, 128.27, 127.90, 125.19, 122.48, 121.29, 121.13, 116.70(CH_3*C*N), 69.28(*C*$_5H_4$), 69.07(*C*$_5H_4$), 66.25(*C*$_5H_4$), 64.72(*C*$_5H_4$), 28.36(*C*H(CH_3)$_2$), 28.10(*C*H(CH_3)$_2$), 22.70(CH(*C*H_3)$_2$), 22.66(CH(*C*H_3)$_2$), 22.38(CH(*C*H_3)$_2$), 21.95(N=C*Me*), 20.66(N=C*Me*), 19.10(*C*H_3CN), 6.08(Pd-*C*H_3). ESI-MS (m/z): calcd for $[C_{51}H_{62}Fe_2N_3Pd]^+$ 934.2677 found: 934.2684. Anal. Calcd for $[C_{51}H_{62}Fe_2N_3Pd]^+$ $[C_{32}H_{12}BF_{24}]^-$: C, 55.43; H, 4.15; N, 2.34; Found: C, 55.69; H, 4.13; N, 2.33.

Procedure for the synthesis of pre-isolated oxidized catalysts

[Pd-CN]$^+$: A 50 mL Schlenk flask was charged with complex **Pd-CN** (180 mg, 0. 1 mmol), AgBAF (95.1 mg, 0.1 mmol) and 20 mL CH_2Cl_2. The mixture was stirred for 1 h. The resulting mixture was filtered through Celite to remove the Ag precipitate, dried under vacuum and submitted to the polymerization and copolymerization procedure without further purification.

[Pd-CN]$^{2+}$: A 50 mL Schlenk flask was charged with complex **Pd-CN** (180 mg, 0. 1 mmol),

AgBAF (190 mg, 0.2 mmol) and 20 mL CH_2Cl_2. The mixture was stirred for 1 h. The resulting mixture was filtered through Celite to remove the Ag precipitate, dried under vacuum and submitted to the polymerization and copolymerization procedure without further purification.

Procedure for the Synthesis of Pd carbonyl complexes.

A 10 mL Schlenk flask was charged with 30.0 μmol of the Pd complex, NaBAF (30.0 μmol) and 5.0 mL of dry CH_2Cl_2. The solution was stirred for 10-60 min under a balloon of CO, leading to darkening and increase in turbidity of the solution. The mixture was filtered through Celite and concentrated in vacuo to afford the desired complexes.

Procedure for ethylene homopolymerization.

In a typical experiment, a 350 mL glass thick-walled pressure vessel was charged with 20 mL toluene and a magnetic stir bar in the glovebox. The pressure vessel was connected to a high pressure line and the solution was degassed. The vessel was warmed to the desired temperature using an oil bath and allowed to equilibrate for 5 min. 10 μmol of Pd complex in 2 mL CH_2Cl_2 was injected into the polymerization system via syringe. With rapid stirring, the reactor was pressurized and maintained at 8.0 atm of ethylene. After 3 h, the pressure vessel was vented and the polymer was quenched with Methanol and dried for 24 h under vacuum.

Analysis of Polymer Branching by ^{13}C NMR Spectroscopy. $B= 1000\times I_{BMe}/I_{total}$. $1B1\%=I_{Me\text{-}sec}/I_{Me}$.

General in-Situ-Oxidized Polymerization Procedure by palladium complexes.

Under an inert atmosphere, a Fisher Porter bottle was charged with AgBAF 10/20 μmol, 20 mL of toluene, and a magnetic stir bar. The bottle was sealed and placed in an oil bath at the desired temperature. The vessel was pressurized with ethylene and allowed to equilibrate under constant pressure for 5 minutes with stirring. 10 μmol of Pd-CN complex in 2 mL CH_2Cl_2 was injected into the polymerization system via syringe. With rapid stirring, the reactor was pressurized and maintained at 8.0 atm of ethylene. After 3 h, the pressure vessel was vented and the polymer was quenched with Methanol and dried for 24 h under vacuum.

Procedure for E-MA copolymerization.

In a typical experiment, a 150 mL glass thick-walled pressure vessel was charged with toluene, a desired amount of MA and a magnetic stir bar in the glovebox. The pressure vessel was connected to a high pressure line and the solution was degassed. The vessel was warmed to 40 □ using an oil bath and allowed to equilibrate for 5 min. 10 μmol of Pd complex in 2 mL CH_2Cl_2 was injected into the polymerization system via syringe. With rapid stirring, the reactor was pressurized and maintained at 1.0 atm of ethylene. After 12 h, the pressure vessel was vented and the resulting mixture was filtered through silica gel. After removal of solvent under reduced pressure, the E-MA copolymer was obtained, quenched with Methanol and dried at 80 °C for 24 h under vacuum.

Analysis of MA incorporation (mol %) by ^1H NMR Spectroscopy. $MA\%= 4I_{OMe}/3(I_{CH3}+I_{CH2}+I_{CH}+I_{OMe})\times100\%$. OMe (s, ca. 3.61-3.76 ppm); CH_2 and CH (m, ca. 1.0-1.45 ppm); CH_3 (m, ca. 0.77-0.95 ppm).

Procedure for E-NB, E-NB-Ac copolymerization.

In a typical experiment, a 350 mL glass thick-walled pressure vessel was charged with toluene, a desired amount of NB or NB-Ac and a magnetic stir bar in the glovebox. The pressure vessel was connected to a high pressure line and the solution was degassed. The

vessel was warmed to 40 □ using an oil bath and allowed to equilibrate for 5 min. 10 μmol of Pd complex in 2 mL CH_2Cl_2 was injected into the polymerization system via syringe. With rapid stirring, the reactor was pressurized and maintained at 8.0 atm of ethylene. After 3 h, the pressure vessel was vented and the resulting mixture was filtered through silica gel. After removal of solvent under reduced pressure, the copolymer was obtained, quenched with Methanol and dried at 80 °C for 24 h under vacuum.

Analysis of NB incorporation (mol %) by ^{13}C NMR Spectroscopy. Calculated according to published procedure.[3]

Analysis of NB-AC incorporation (mol %) by ^{1}H NMR Spectroscopy. NB-AC%= $4I_{COMe}/3(I_{CH3}+I_{CH2}+I_{CH})\times100\%$. COMe (m, ca. 4.88-4.96 ppm); CH_2 and CH (m, ca. 1.0-1.45 ppm); CH_3 (m, ca. 0.77-0.95 ppm).

Polymerization of α-Olefins.

In a typical procedure, a round-bottom Schlenk flask with stirring bar was heated 3 h to150 °C under vacuum and then cooled to room temperature. A proper amount of freshly distilled 1-hexene was introduced into the flask, which contained the required amount of toluene. Polymerization was started by injecting the catalyst solution (10 μmol, 2 mL CH_2Cl_2) into the reactor, and the total volume of solvent was kept at 20 mL. After desired amount of time, the polymerization was terminated by adding 0.2 mL of the Et_3SiH and dried in vacuum at 60 °C to a constant weight.

1-Hexene monitoring experiment.

In a NMR test tube, 0.12 mL (1mmol, 100eq) freshly distilled 1-hexene was introduced, which contained 10μmol catalyst and 1ml $CDCl_3$ as the reaction solvent. Then the test tube was submitted to the NMR test at the temperature of 25□ every 20 minutes.

Electrochemistry

Cyclic voltammetry measurements were performed using 0.01 mmol compound in 5 ml DCM solution (0.002 M) with 0.2 M $^{n}Bu_4NPF_6$ as supporting electrolyte and Ag/AgCl as the reference electrode, along with platinum working and auxiliary electrodes, and a scan rate of 100 mVs^{-1}. The results of the electrochemical studies are shown in Table S1.

Due to the air and moisture sensitivity of the complexes, samples were weighed out in a glovebox, placed under nitrogen in the electrochemical cell, and then dissolved. During the timescale of the experiments no degradation was observed to occur, the solutions remaining orange. Scan rates of 50, 100 and 200 mVs-1 were studied and the set of cyclic voltammograms for compounds are shown in Figure S1-Figure S9.

2. Table, Figures

Table S1. Cyclic Voltammetry data for compound [a]

Compound	Ep^A/V	Ep^C/V	$E_{1/2}$/V
Pd-Cl	0.548	0.384	0.466
Pd-CN	0.589	0.405	0.497
[Pd-CN]$^+$	0.541	0.396	0.469
[Pd-CN]$^{2+}$	0.534	0.392	0.463
AgBAF	0.960	0.620	0.790

[a] Cyclic voltammetry measurements were performed using 0.01 mmol compound in 5 ml DCM solution (0.002 M) with 0.2 M $^nBu_4NPF_6$ as supporting electrolyte and Ag/AgCl as the reference electrode, along with platinum working and auxiliary electrodes, and a scan rate of 100 mVs^{-1}.

Table S2. Branching distributions of the PEs from table 1.[a]

Entry	Branching distribution(/1000C)						Branches (/1000C)[b]
	Me	Et	Pr	^{n}Bu	Hex+	1B1%[b]	
1	33.3	21.2	2.9	10.3	22.2	14.7(±0.8)	88(±1.1)
2	31.5	21.1	2.7	10.6	22.5	18.4(±0.9)	88(±1.4)
3	31.6	22.1	3	9.3	26.1	20.1(±0.4)	92(±2.3)
4	30.3	20.9	2.2	12.5	21.6	15.2(±0.3)	88(±1.6)
5	28.7	20.4	2.7	13.3	21.1	18.1(±0.8)	89(±1.1)
6	30.1	22	2.4	11.6	25.3	19.3(±1.0)	91(±1.9)
7	30.5	21.9	2	12.2	20.8	15.5(±0.9)	87(±2.2)
8	30.4	21.8	2.3	11.4	22.1	16.6(±1.1)	88(±0.9)
9	30.8	23	2.3	11.5	25.5	20.4(±1.3)	91(±2.6)

[a]Sample from Table 1, entries 1-9. Measured by ^{13}CNMR in $CDCl_3$, r.t. For this measurement, we define a branch length as the number of carbons from and including a methyl to the nearest methine, including the intervening methylenes; thus, one *sec*-butyl branch would contribute one methyl and one ethyl branch to the listed total of ethyl and methyl branches as referenced by Cotts's previous work.[4]

[b]Reported values are averages over multiple trials.

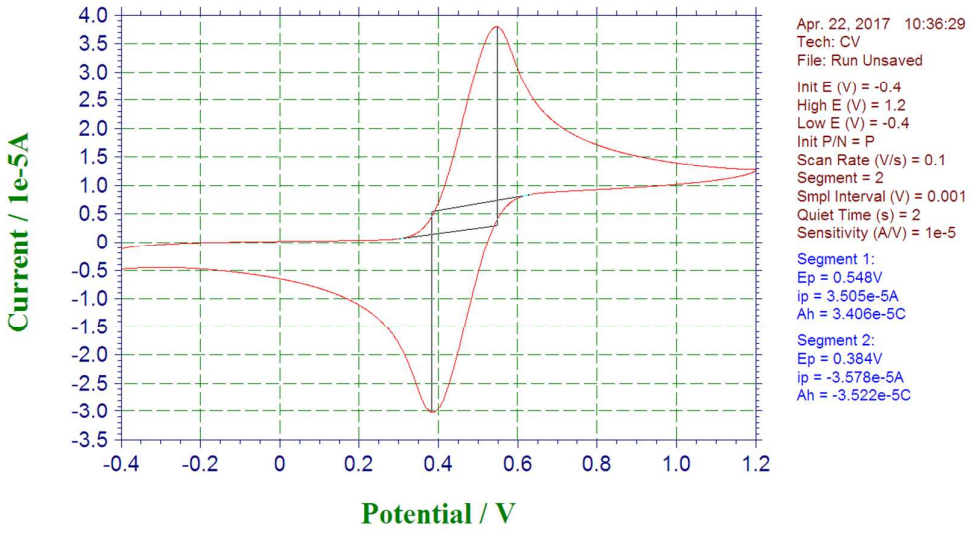

Figure S1. Cyclic Voltammogram of **Pd-Cl** at scan rate of 100 mVs^{-1}.

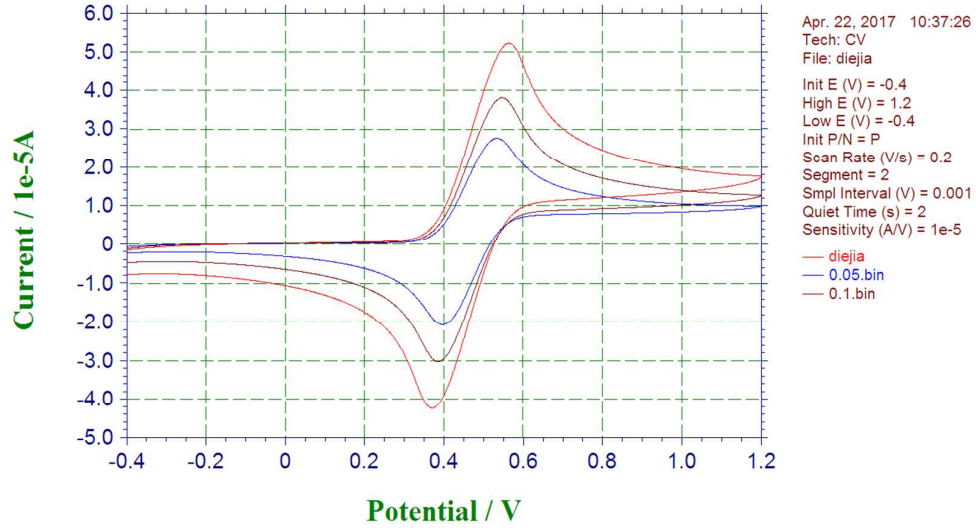

Figure S2. Cyclic Voltammogram of **Pd-Cl** at different scan rates from 50 mVs^{-1} to 100 mVs^{-1} to 200 mVs^{-1}.

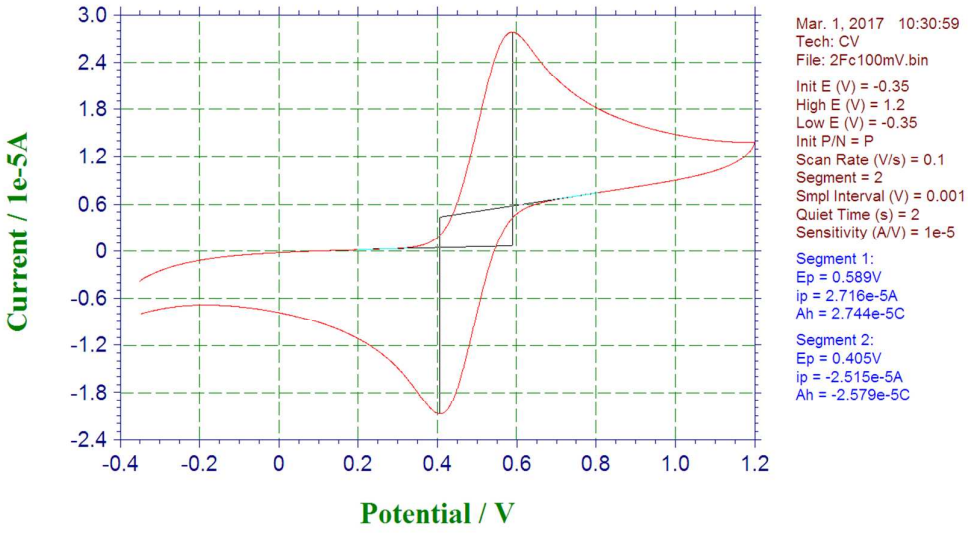

Figure S3. Cyclic Voltammogram of **Pd-CN** at scan rate of 100 mVs^{-1}

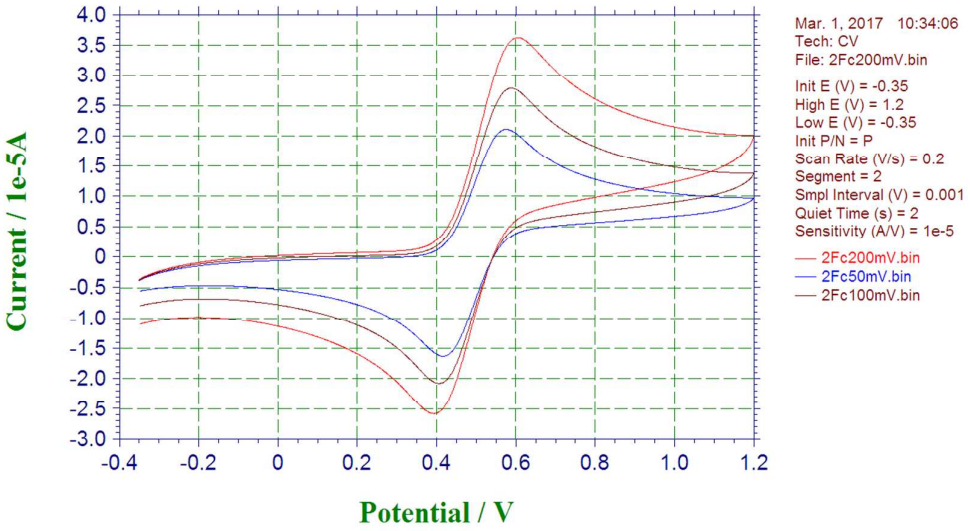

Figure S4. Cyclic Voltammogram of **Pd-CN** at different scan rates from 50 mVs^{-1} to 100 mVs^{-1} to 200 mVs^{-1}.

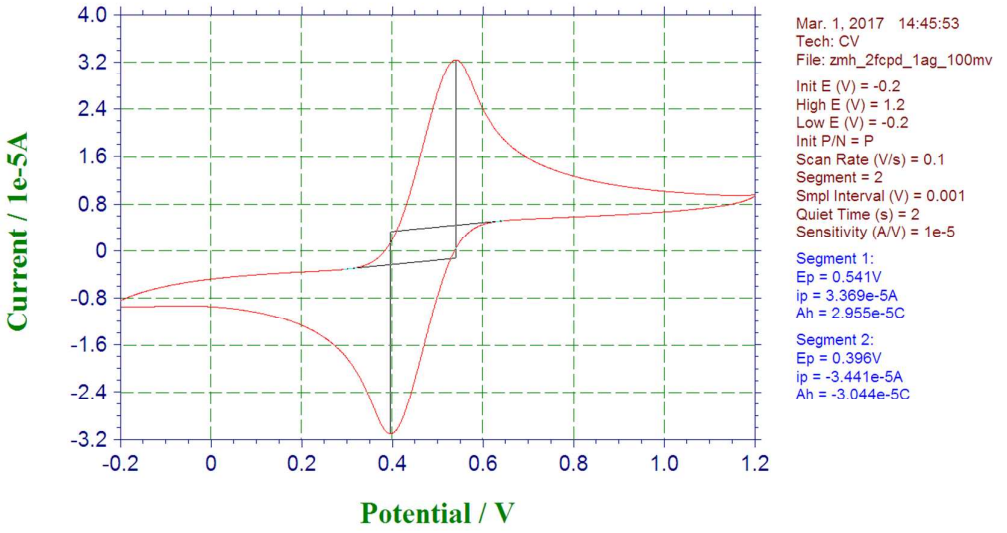

Figure S5. Cyclic Voltammogram of **[Pd-CN]**$^{+}$ at scan rate of 100 mVs^{-1}.

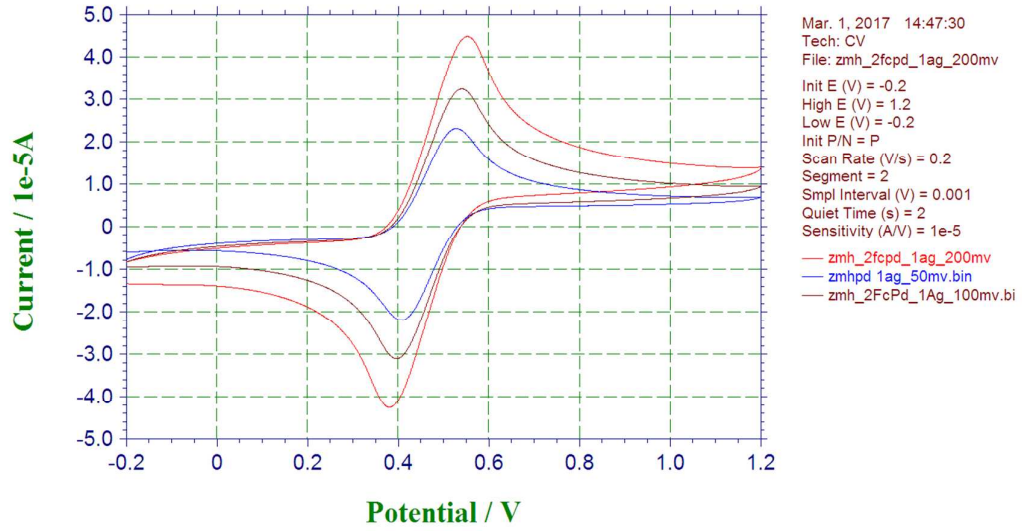

Figure S6. Cyclic Voltammogram of **[Pd-CN]**$^{+}$ at different scan rates from 50 mVs^{-1} to 100 mVs^{-1} to 200 mVs^{-1}.

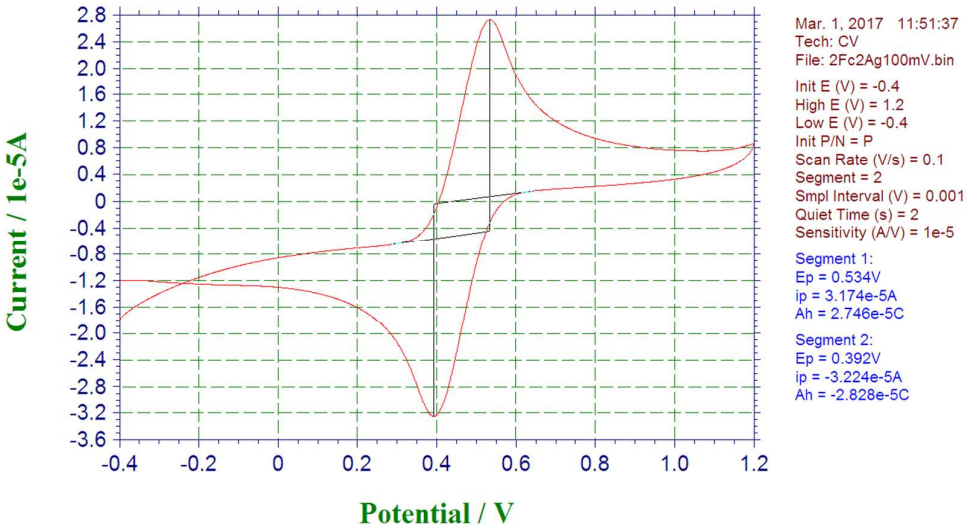

Figure S7. Cyclic Voltammogram of **[Pd-CN]**$^{2+}$ at scan rate of 100 mVs^{-1}

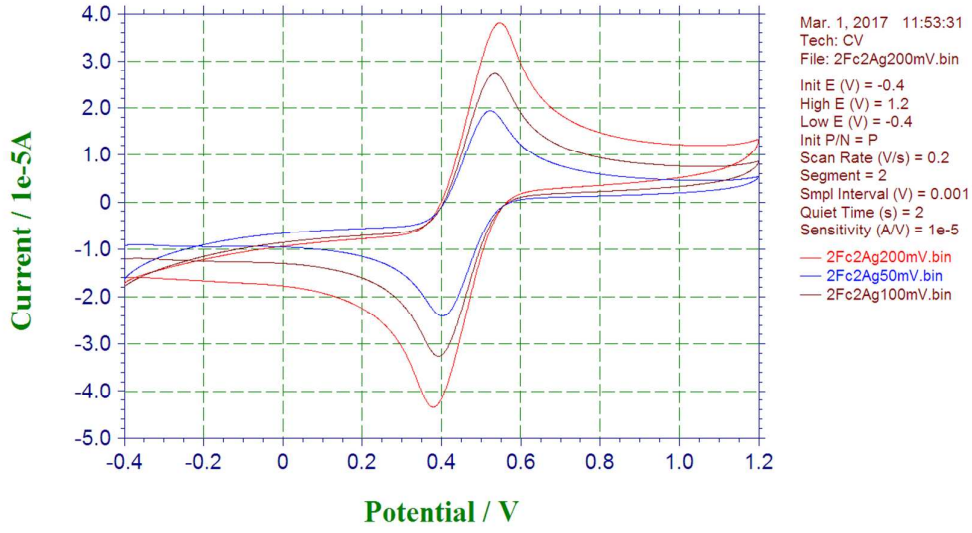

Figure S8. Cyclic Voltammogram of **[Pd-CN]**$^{2+}$ at different scan rates from 50 mVs^{-1} to 100 mVs^{-1} to 200 mVs^{-1}.

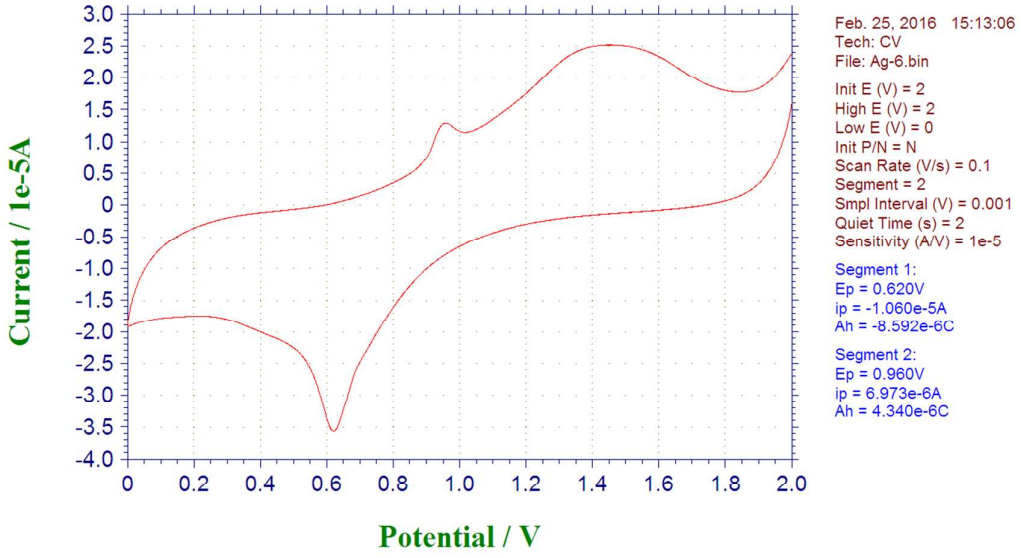

Figure S9. Cyclic Voltammogram of **AgBAF** at scan rate of 100 mVs^{-1}

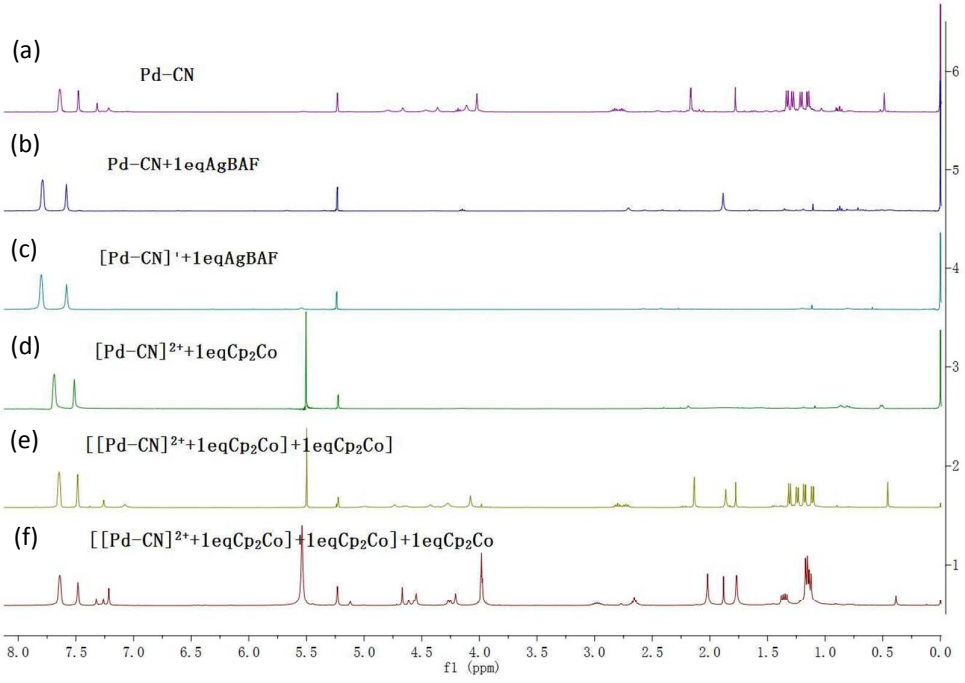

Figure S10. ^{1}H NMR stack (CD_2Cl_2) showing the complete disappearance of the signals and the reappearance of the NMR signals. (a) **Pd-CN**; (b) **Pd-CN** + 1 eq. AgBAF; (c) **Pd-CN** + 2 eq. AgBAF; (d) **Pd-CN** + 2 eq. AgBAF + 1 eq. Cp_2Co; (e) regeneration of **Pd-CN** from **Pd-CN** + 2 eq. AgBAF + 2 eq. Cp_2Co; (f) **Pd-CN** + 2 eq. AgBAF + 3 eq. Cp_2Co, which showed that the **Pd-CN** complex can be reduced by Cp_2Co to some new species.

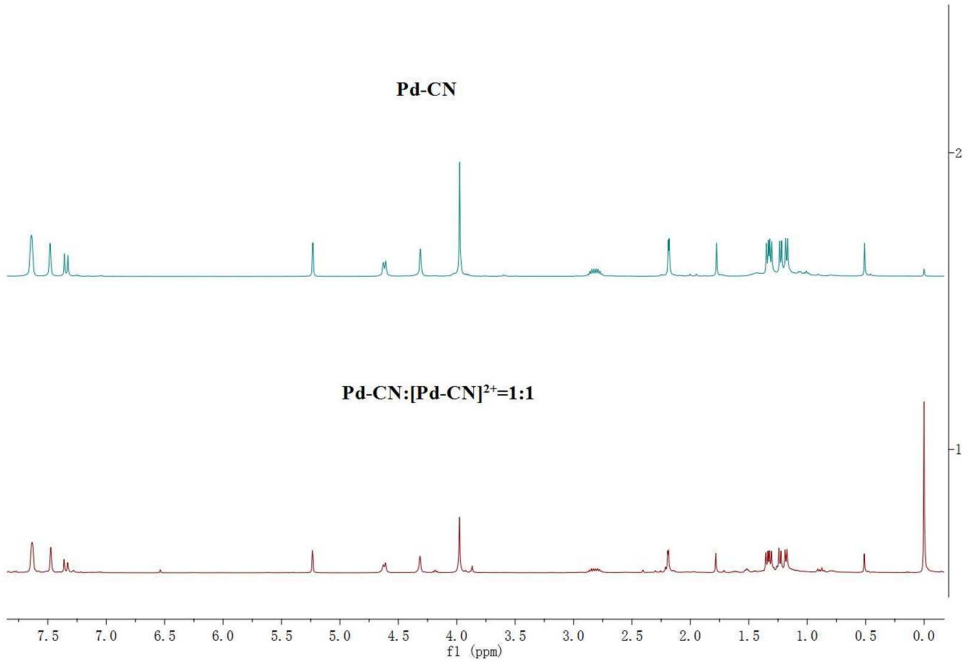

Figure S11. ^{1}H NMR stack (CD_2Cl_2) of **Pd-CN** and a 1:1 mixture of pre-isolated **[Pd-CN]$^{2+}$** and **Pd-CN**.

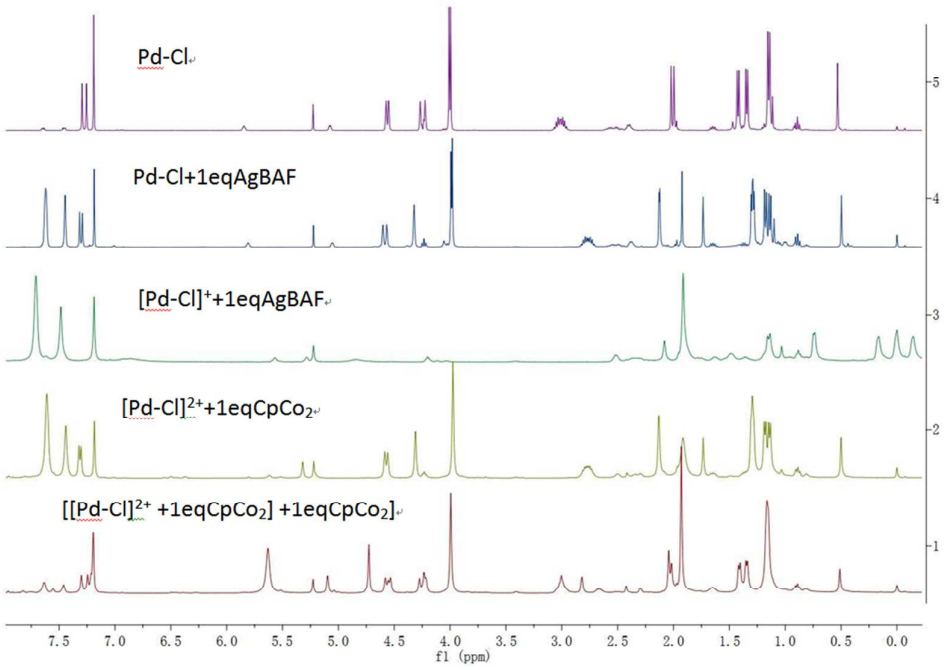

Figure S12. ^{1}H NMR stack ($CDCl_3$) showing the shifting and broadening of the signals, complete disappearance of the signals and the reappearance of the NMR signals.

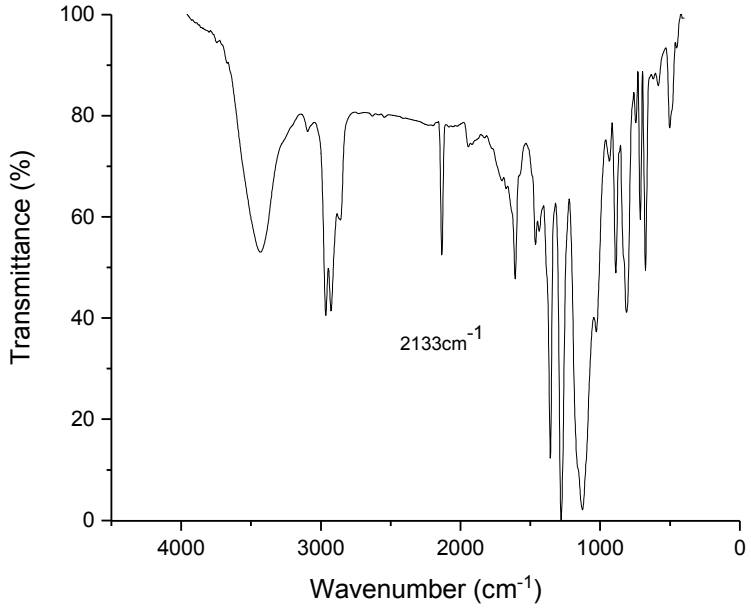

Figure S13. IR of **Pd-CO**. FT-IR spectra were performed on a Bruker VECTOR-22 IR spectrometer. The spectra of all samples were collected at 64 scans with a spectral resolution of 4 cm^{-1} by the KBr disk method.

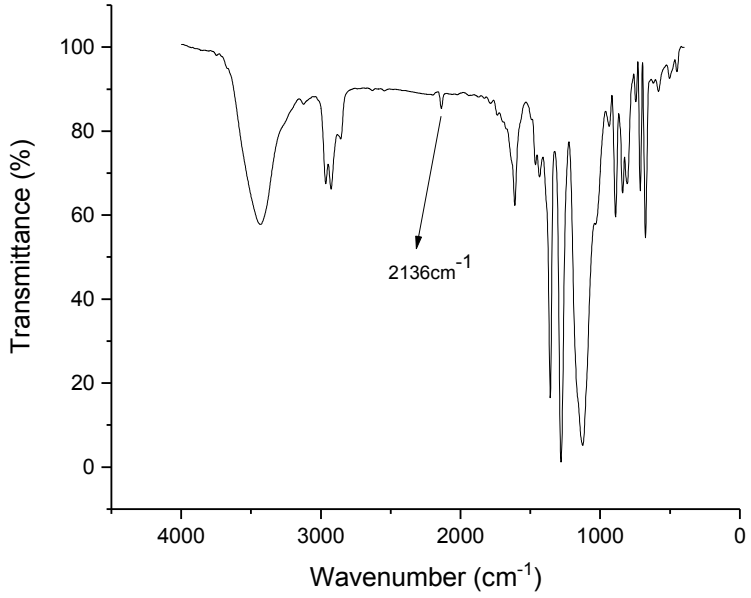

Figure S14. IR of **[Pd-CO]**$^{+}$.

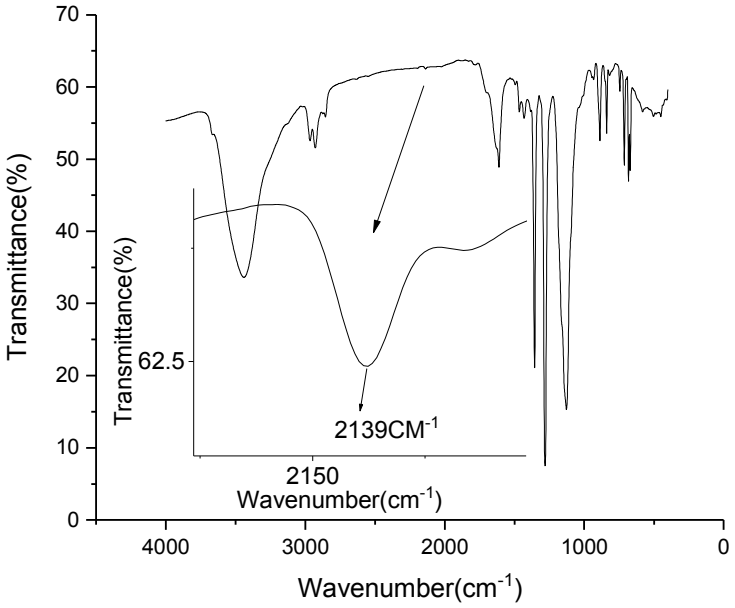

Figure S15. IR of **[Pd-CO]$^{2+}$**. The signal is small for this case, which is due to the decomposition of this oxidized complex. However, The peak at 2139 cm^{-1} is in the range for previously reported α-diimine palladium carbonyl and α-diimine platinum carbonyl species.[5]

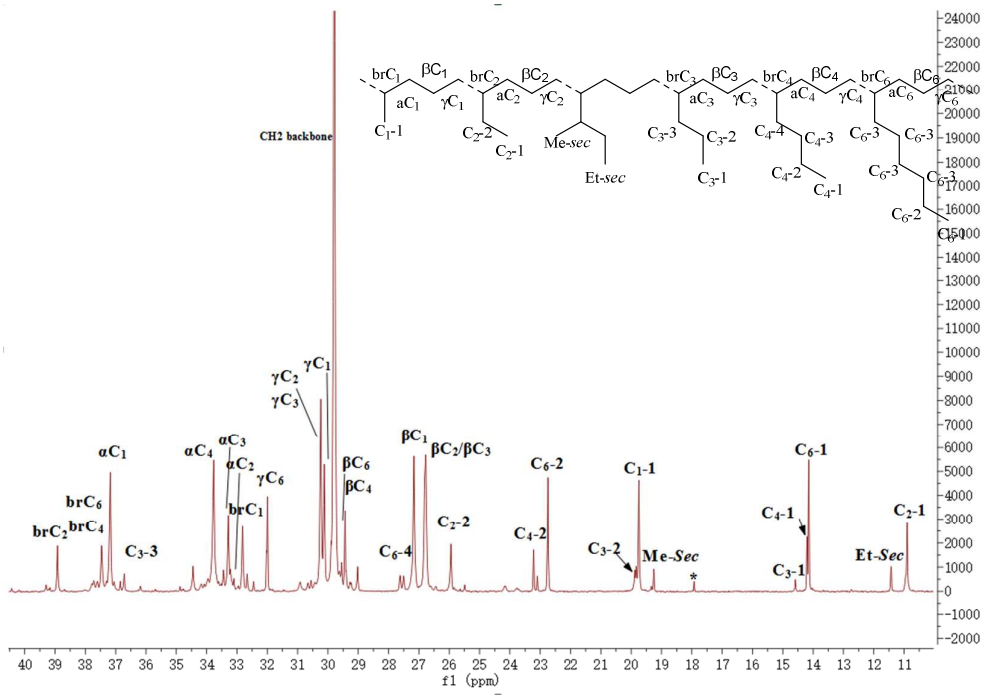

Figure S16. ^{13}C NMR spectrum of the polymer from table 1, entry 7 ($CDCl_3$, r.t.).

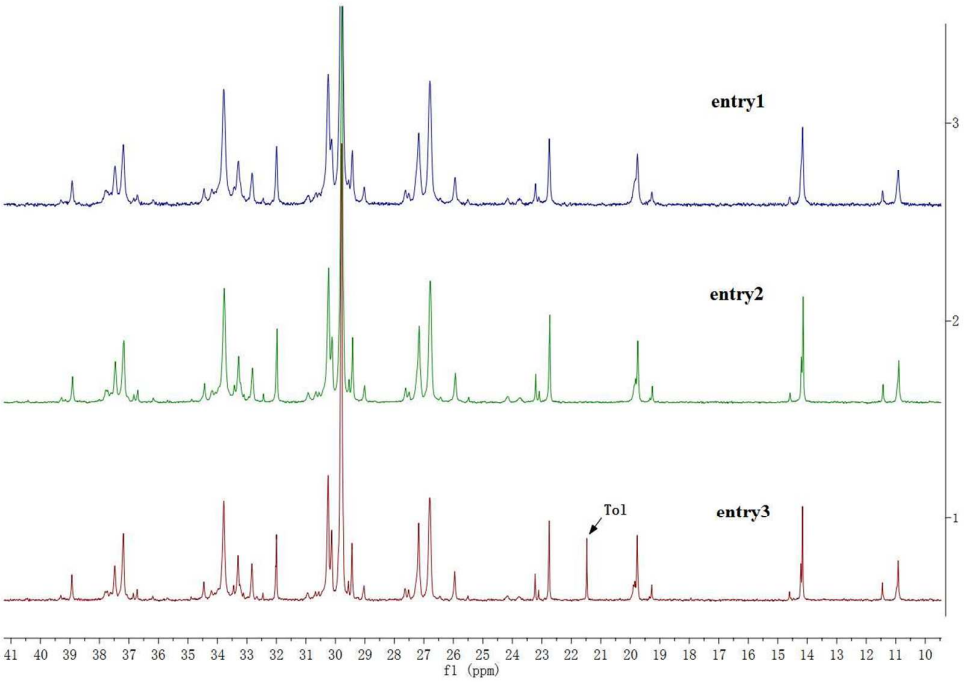

Figure S17. ^{13}C NMR spectrum of the polymer from table 1, entry 1-3 ($CDCl_3$, r.t.).

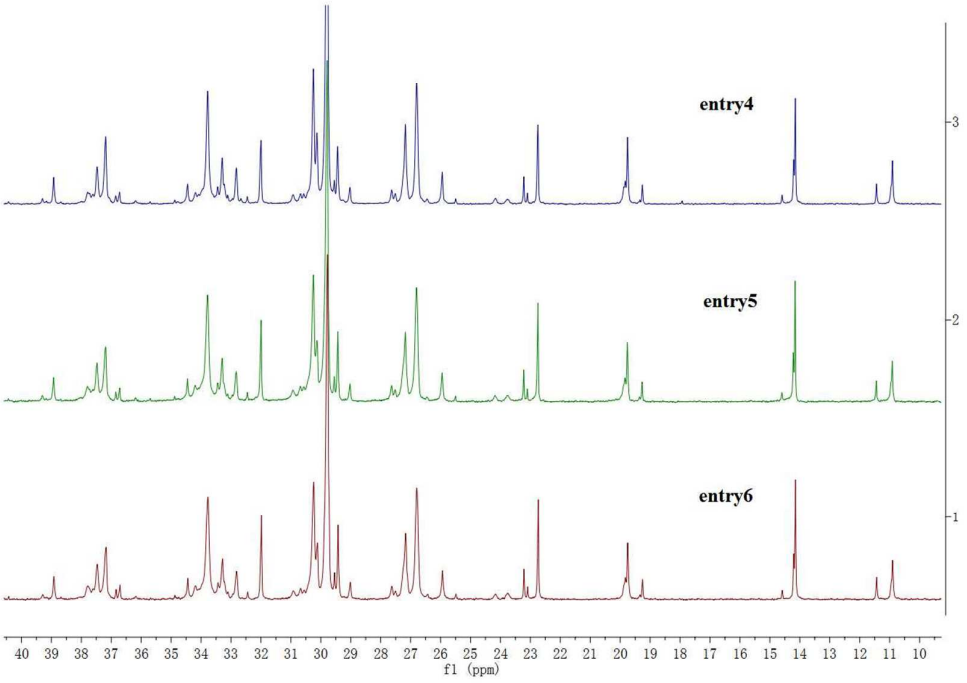

Figure S18. ^{13}C NMR spectrum of the polymer from table 1, entry 4-6 ($CDCl_3$, r.t.).

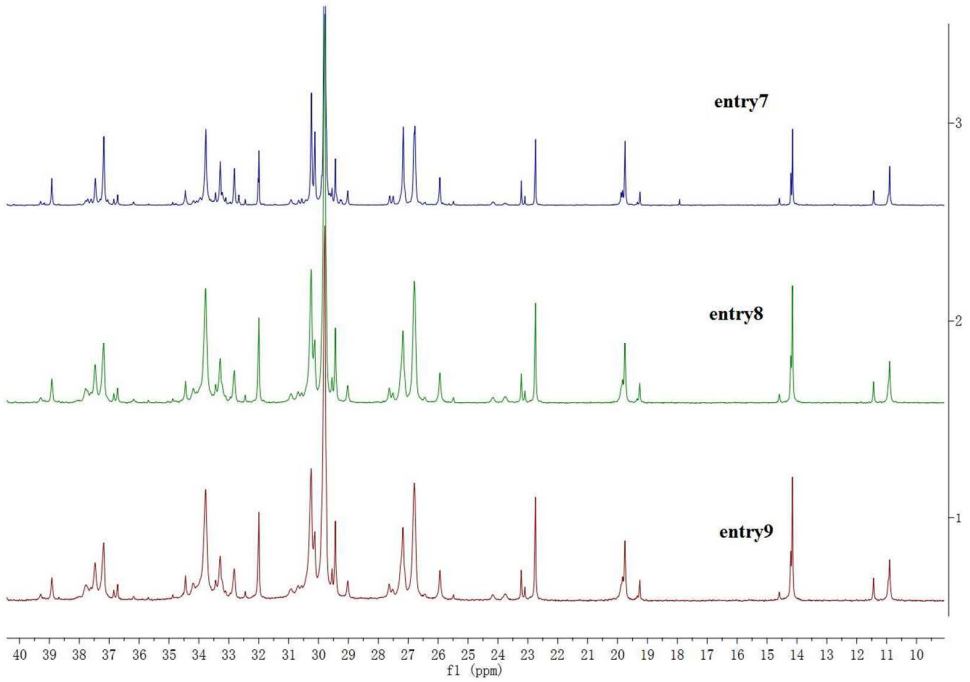

Figure S19. ^{13}C NMR spectrum of the polymer from table 1, entry 7-9 ($CDCl_3$, r.t.).

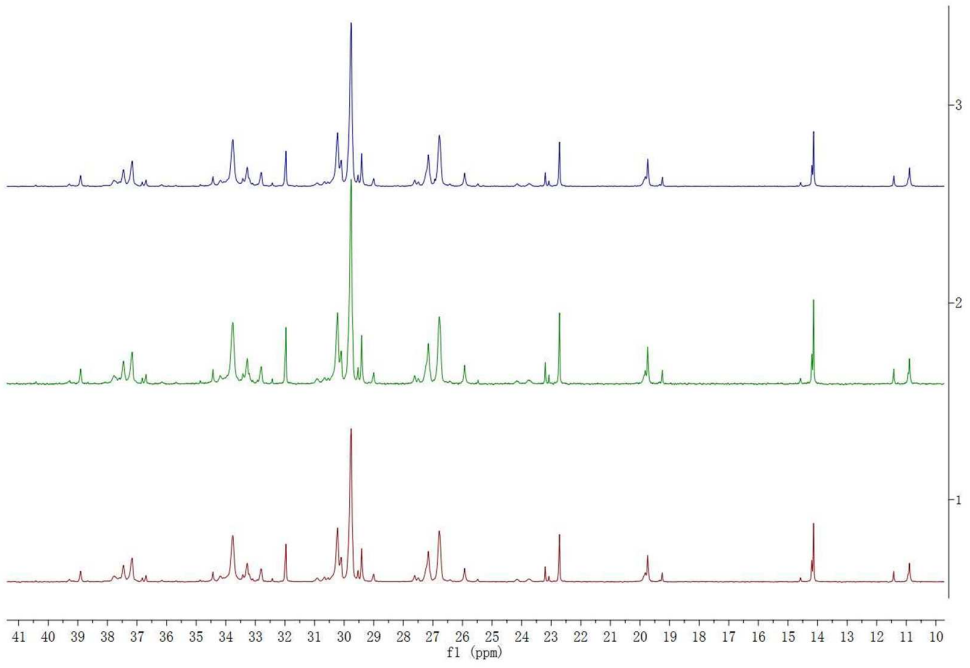

Figure S20. Triple trials of ^{13}C NMR spectrum of the polymer from table S2, entry 1 ($CDCl_3$, r.t.) for determination of *Sec*-Bu Branching distribution(/1000C).

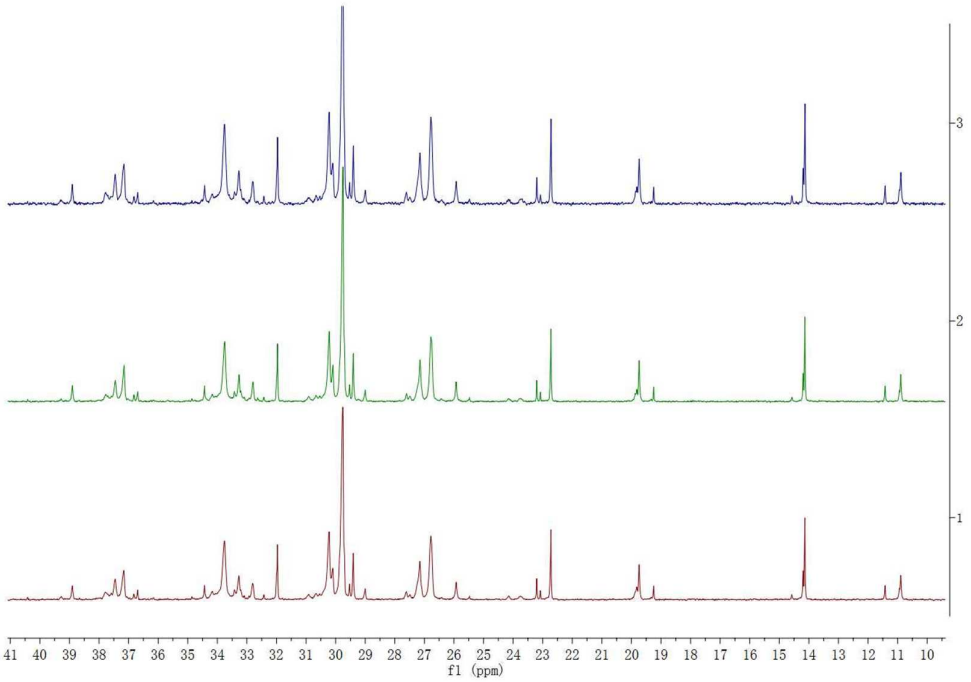

Figure S21. Triple trials of ^{13}C NMR spectrum of the polymer from table S2, entry 2 ($CDCl_3$, r.t.) for determination of *Sec*-Bu Branching distribution(/1000C).

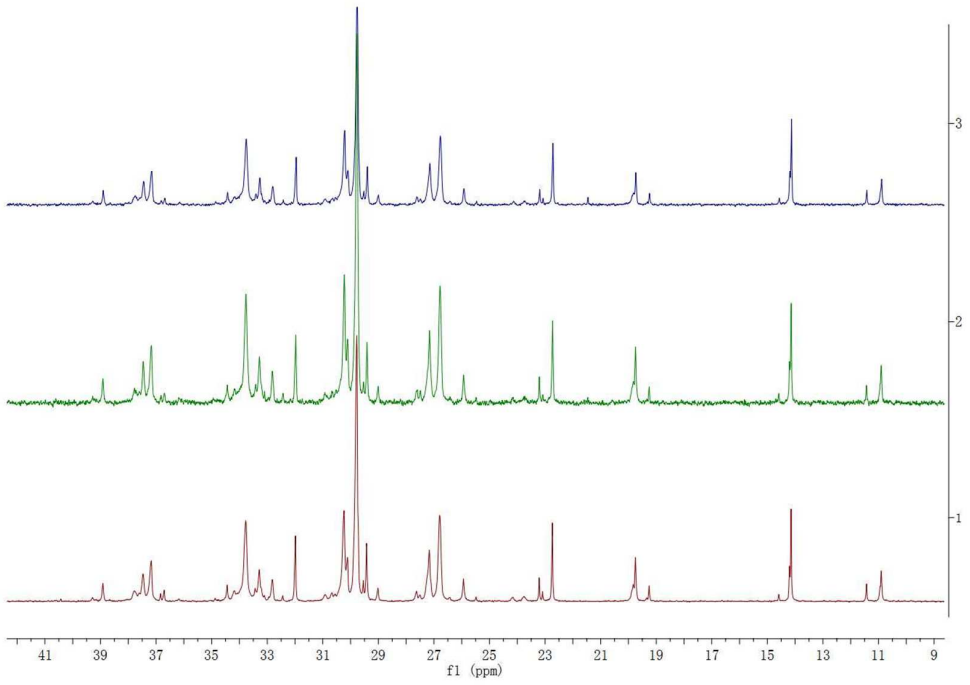

Figure S22. Triple trials of ^{13}C NMR spectrum of the polymer from table S2, entry 3 ($CDCl_3$, r.t.) for determination of *Sec*-Bu Branching distribution(/1000C).

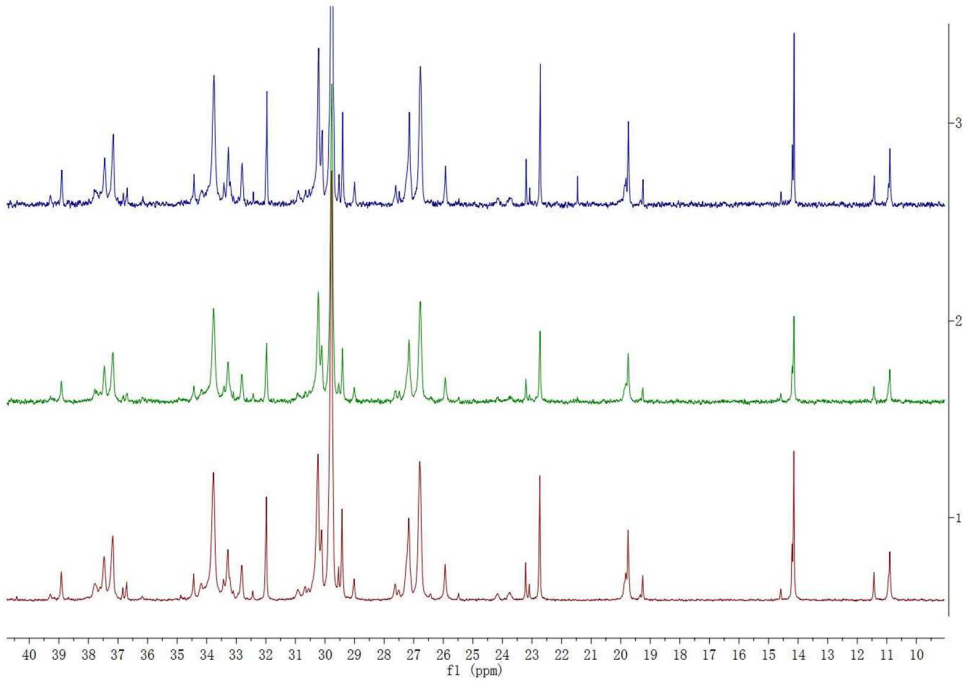

Figure S23. Triple trials of ^{13}C NMR spectrum of the polymer from table S2, entry 4 ($CDCl_3$, r.t.) for determination of *Sec*-Bu Branching distribution(/1000C).

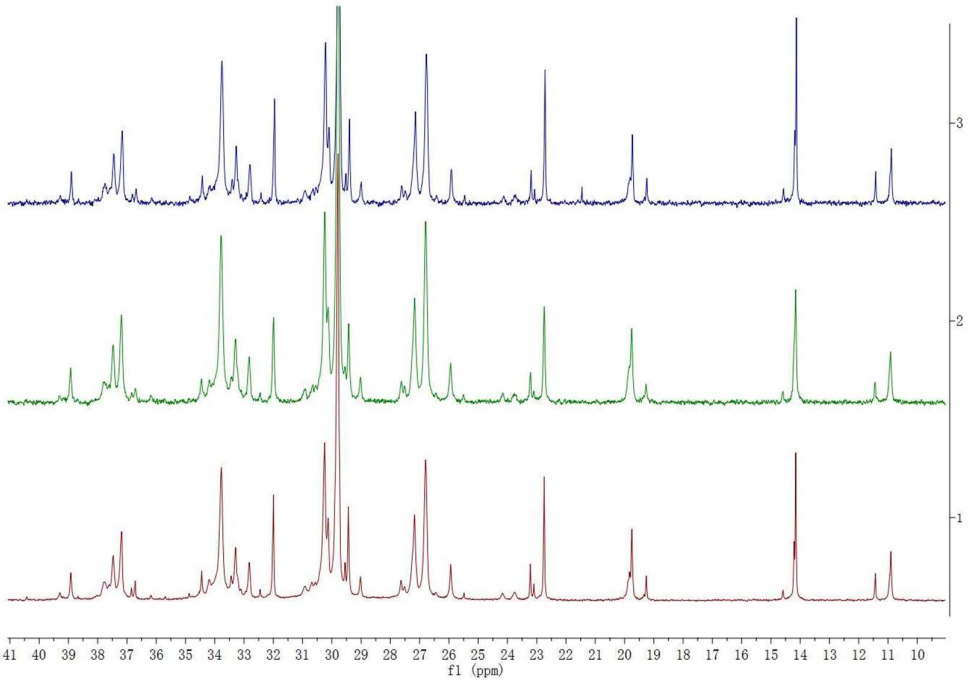

Figure S24. Triple trials of ^{13}C NMR spectrum of the polymer from table S2, entry 5 ($CDCl_3$, r.t.) for determination of *Sec*-Bu Branching distribution(/1000C).

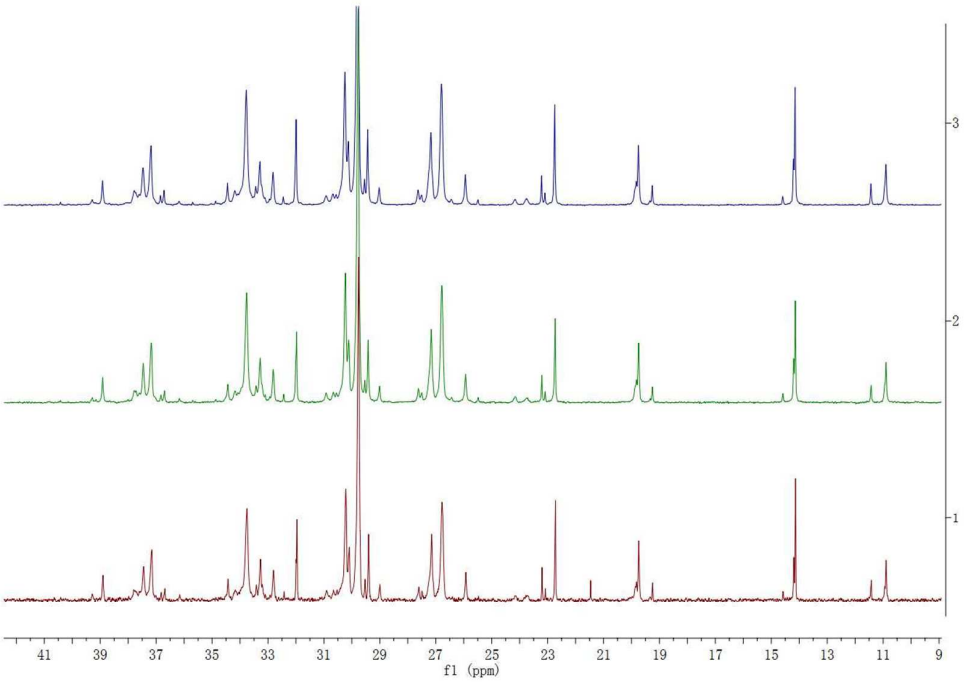

Figure S25. Triple trials of ^{13}C NMR spectrum of the polymer from table S2, entry 6 ($CDCl_3$, r.t.) for determination of *Sec*-Bu Branching distribution(/1000C).

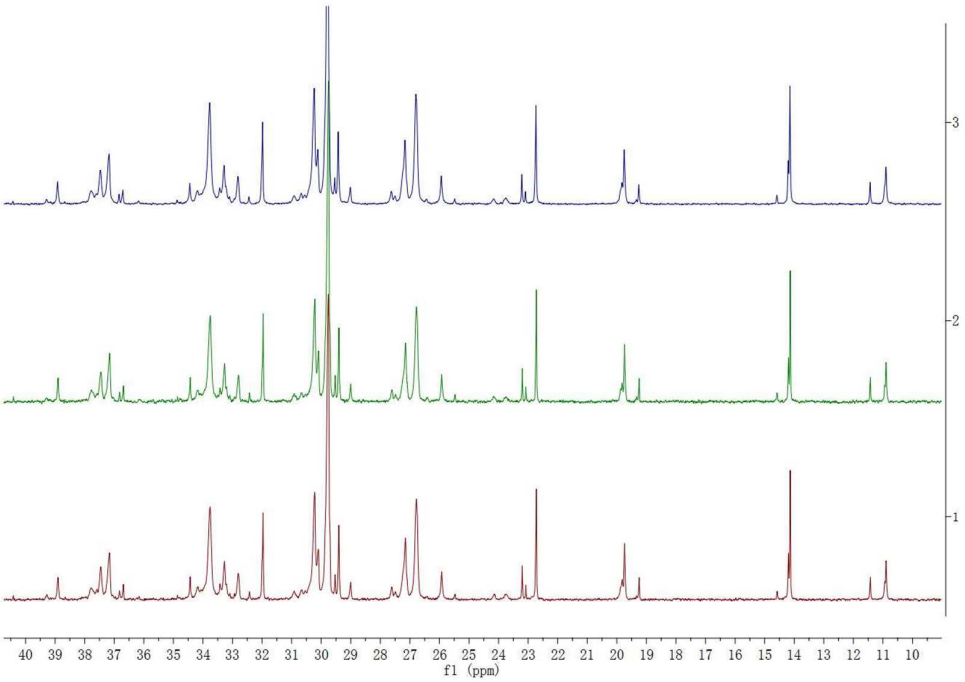

Figure S26. Triple trials of ^{13}C NMR spectrum of the polymer from table S2, entry 7 ($CDCl_3$, r.t.) for determination of *Sec*-Bu Branching distribution(/1000C).

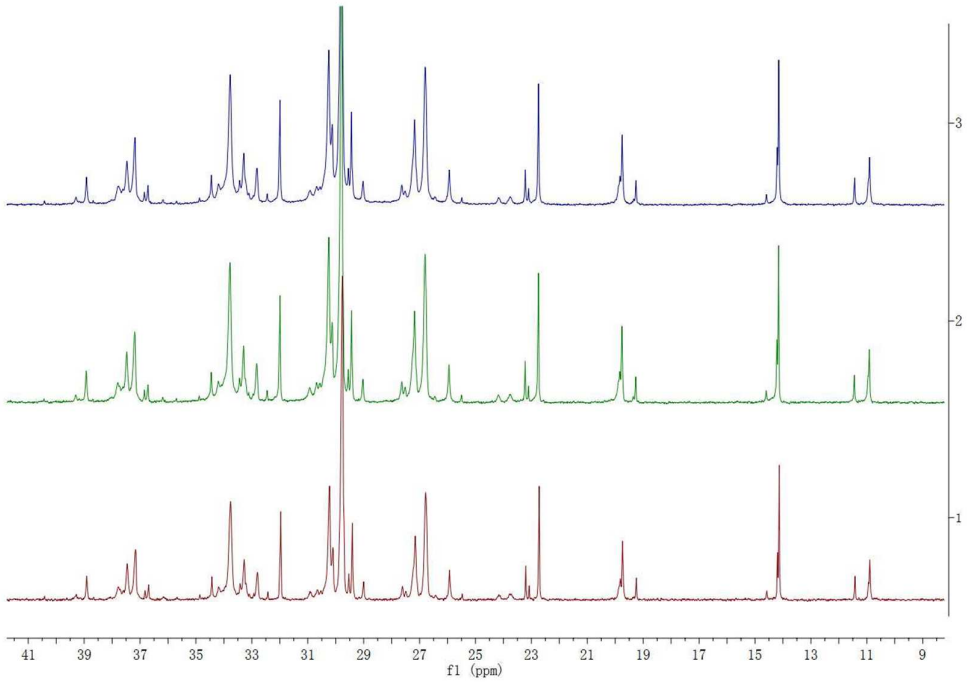

Figure S27. Triple trials of ^{13}C NMR spectrum of the polymer from table S2, entry 8 ($CDCl_3$, r.t.) for determination of *Sec*-Bu Branching distribution(/1000C).

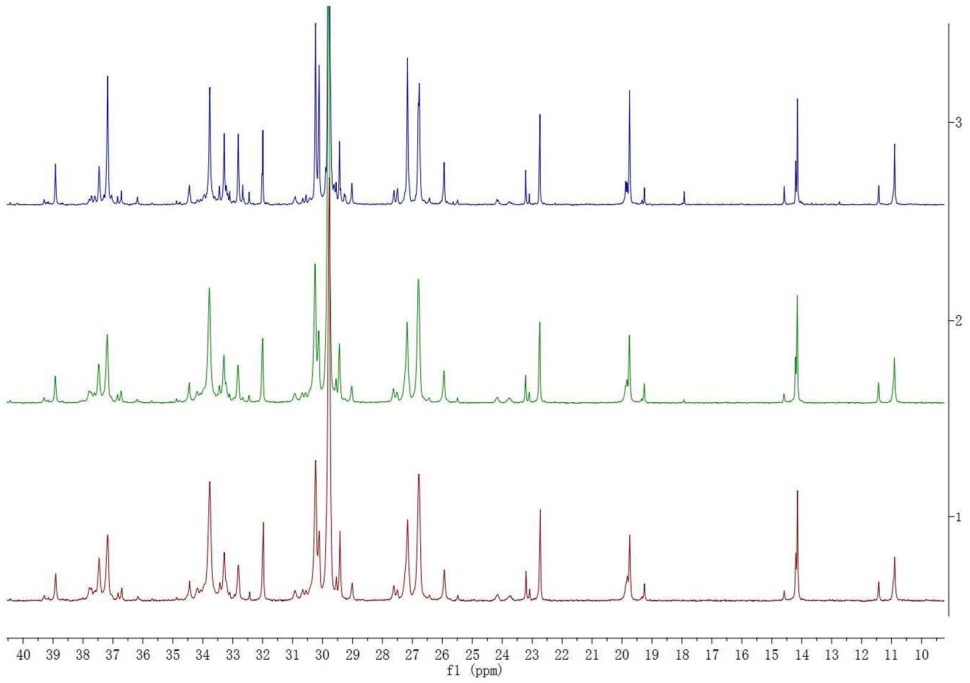

Figure S28. Triple trials of ^{13}C NMR spectrum of the polymer from table S2, entry 9 ($CDCl_3$, r.t.) for determination of *Sec*-Bu Branching distribution(/1000C).

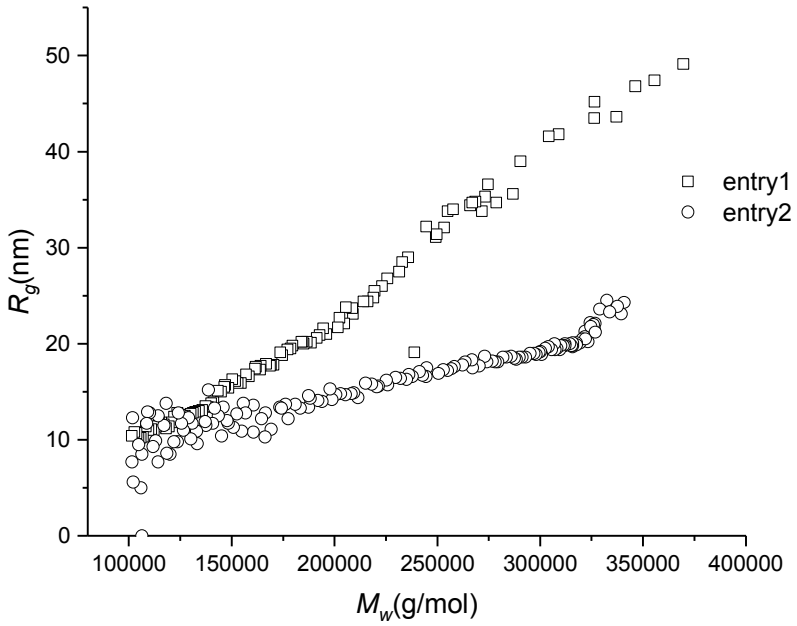

Figure S29. Logarithmetic plot of R_g versus M_w for polyethylenes from Table 1, entries 1 and 2.The distribution of entry 3 and the lower half of the distribution has been omitted, since Rg could not be estimated at these low M_w.

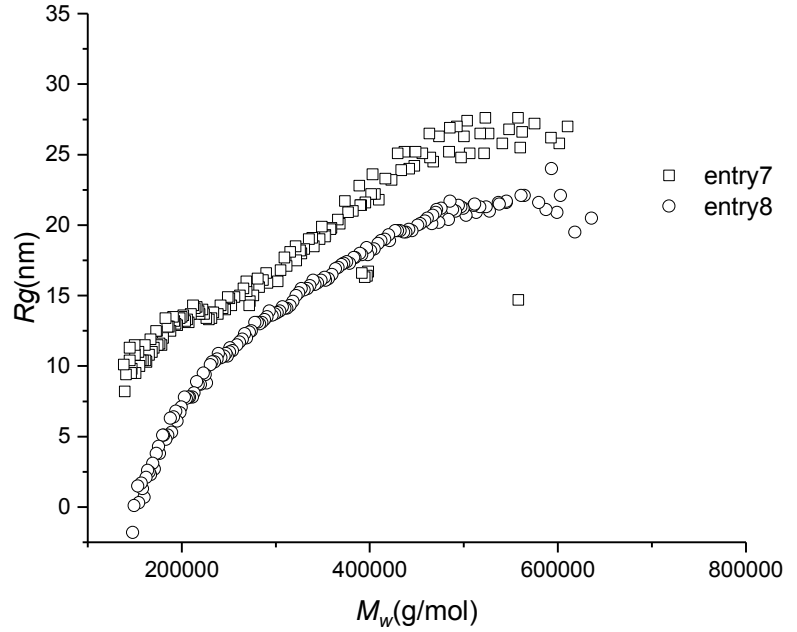

Figure S30. Logarithmetic plot of R_g versus M_w for polyethylenes from Table1, entries 7 and 8. The distribution of entry 9 and the lower half of the distribution has been omitted, since Rg could not be estimated at these low M_w.

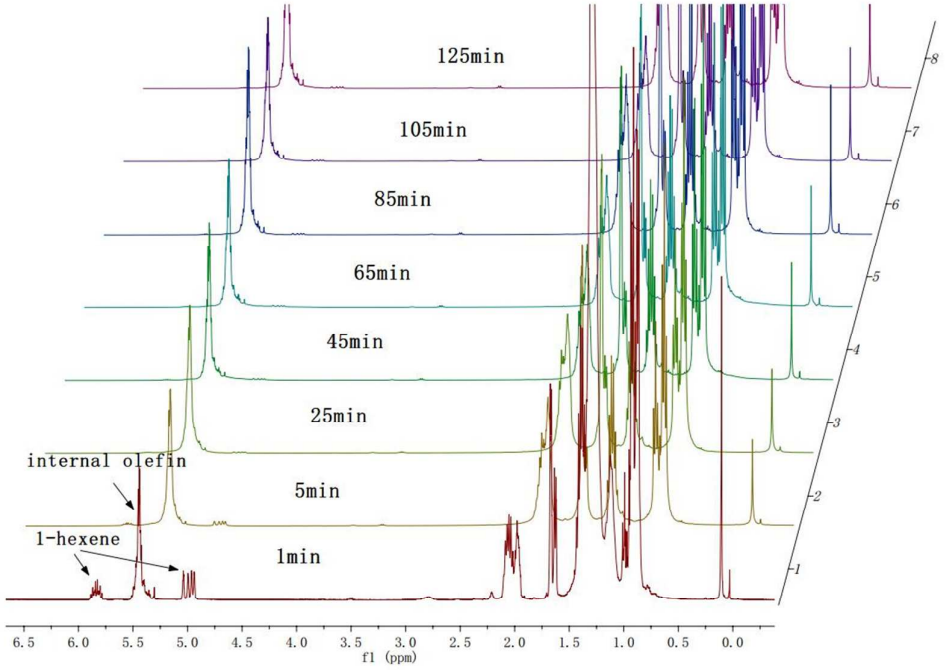

Figure S31. ^{1}H NMR of 1-Hexene polymerization from **Pd-CN** catalyst.

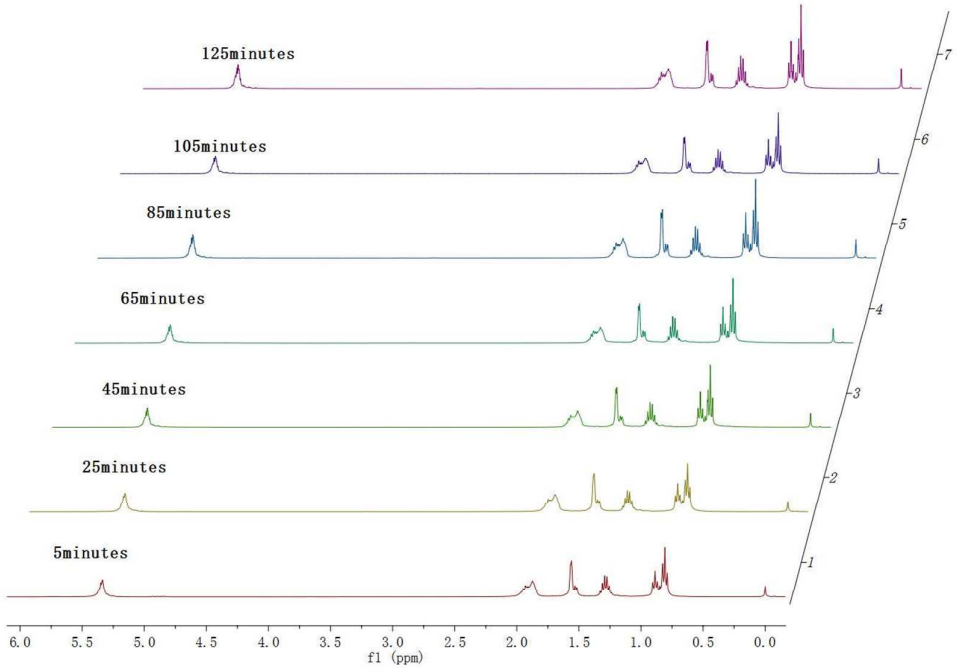

Figure S32. ^{1}H NMR of 1-Hexene polymerization from **[Pd-CN]$^{2+}$** catalyst.

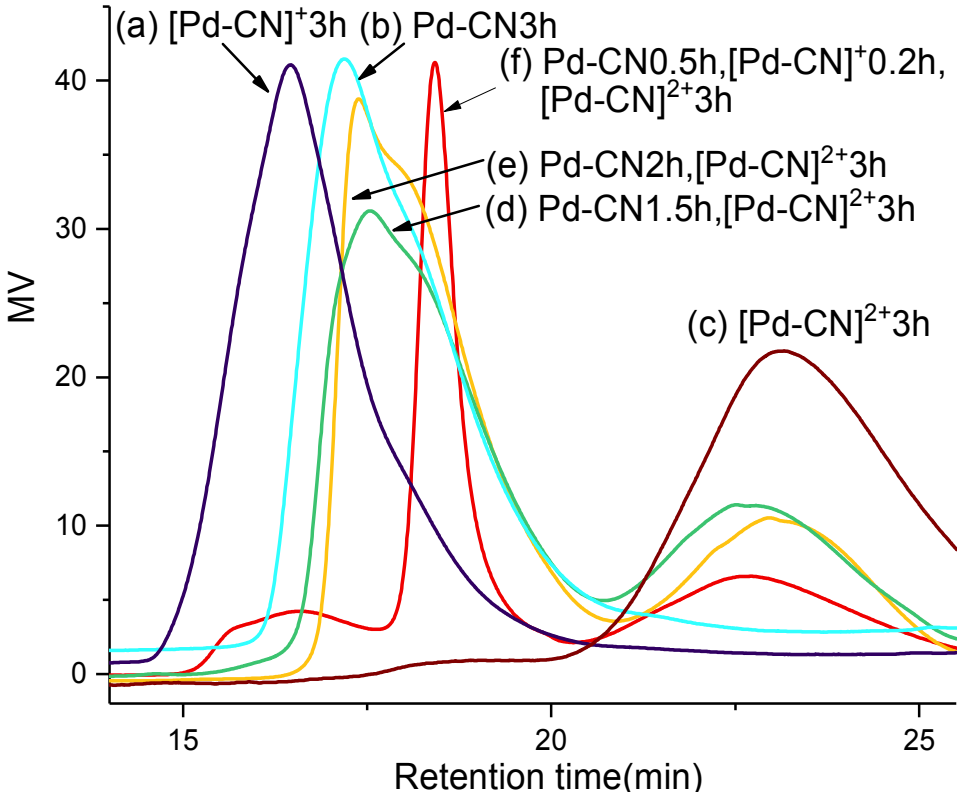

Figure S33. Stepwise and *in-situ* redox control of polyethylene polydispersity. In the current system, the **Pd-CN**, **[Pd-CN]**$^{+}$, and **[Pd-CN]**$^{2+}$ catalysts gave unimodal polyethylene-GPC curves (Figures S33a, S33b and S33c). After a certain amount of time (1.5 or 2 h) during the **Pd-CN**-catalyzed ethylene polymerization, 2.1 equiv. of AgBAF was added to the polymerization solution *in situ*, and the polymerization was continued for another 3h. The polymeric product exhibited nice bimodal GPC curves that overlapped with those produced by **Pd-CN** and **[Pd-CN]**$^{2+}$ as catalysts **(**Figures S33d and S33e). A trimodal curve was generated by taking advantage of this stepwise oxidation strategy (Figure S33f).

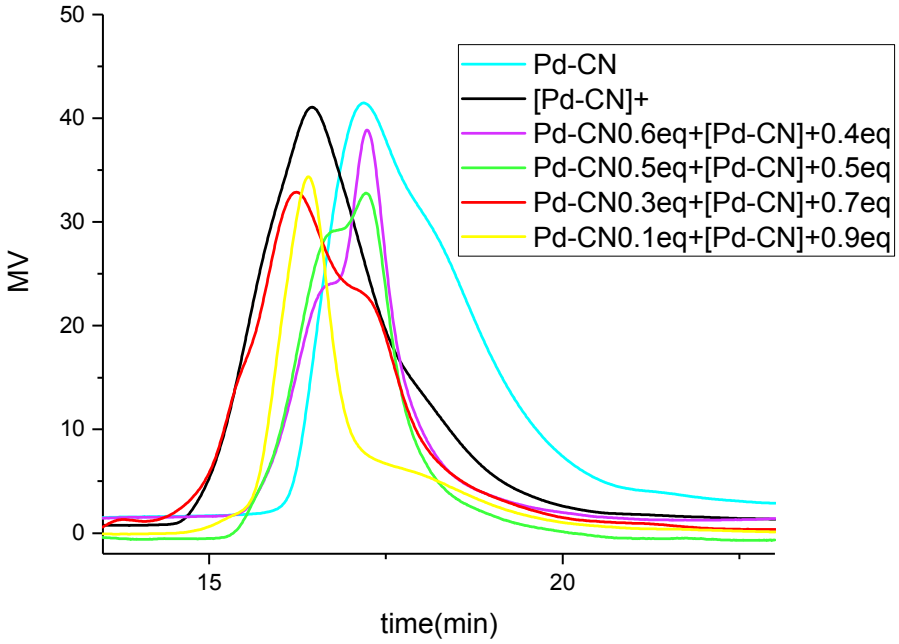

Figure S34. *In-situ* redox control of the polyethylene polydispersity. The partial oxidation of the **Pd-CN** catalyst (addition of 0.x equiv. of AgBAF) leads to a mixture of **Pd-CN** and **[Pd-CN]**$^{+}$, which subsequently produces a polymeric product exhibiting a multi-modal GPC curve.

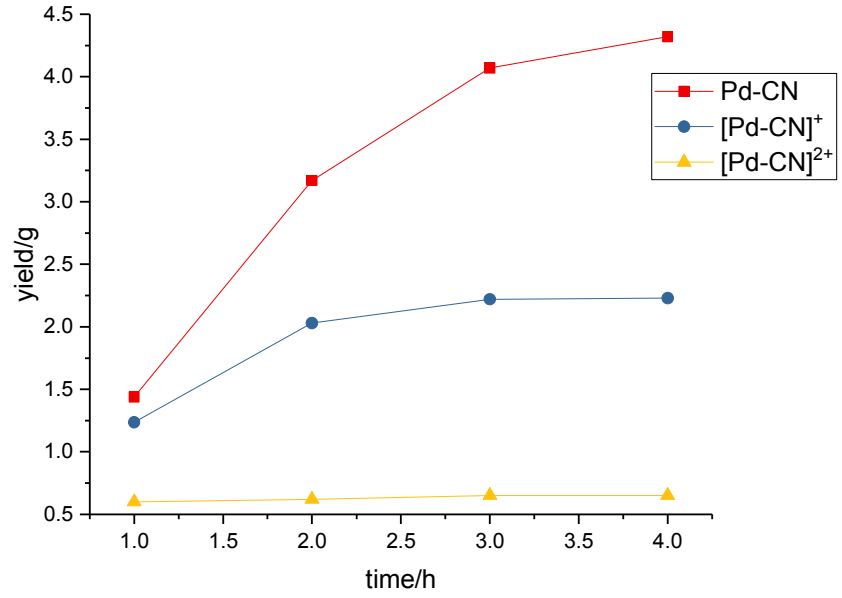

Figure S35. Polyethylene yield versus time for complexes **Pd-CN**, **[Pd_CN]**$^{+}$ and **[Pd_CN]**$^{2+}$ at 40 °C. Conditions: catalyst = 10 μmol, toluene = 20 ml, ethylene = 8 atm.

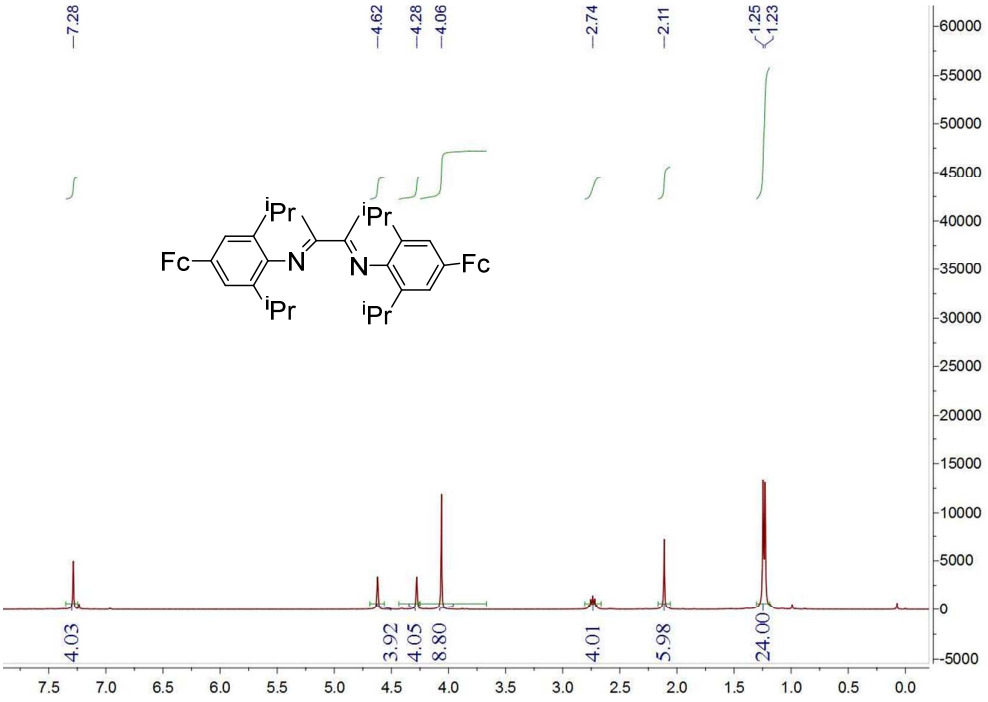

Figure S36. ^{1}H NMR spectrum of **L-Fc** in $CDCl_3$.

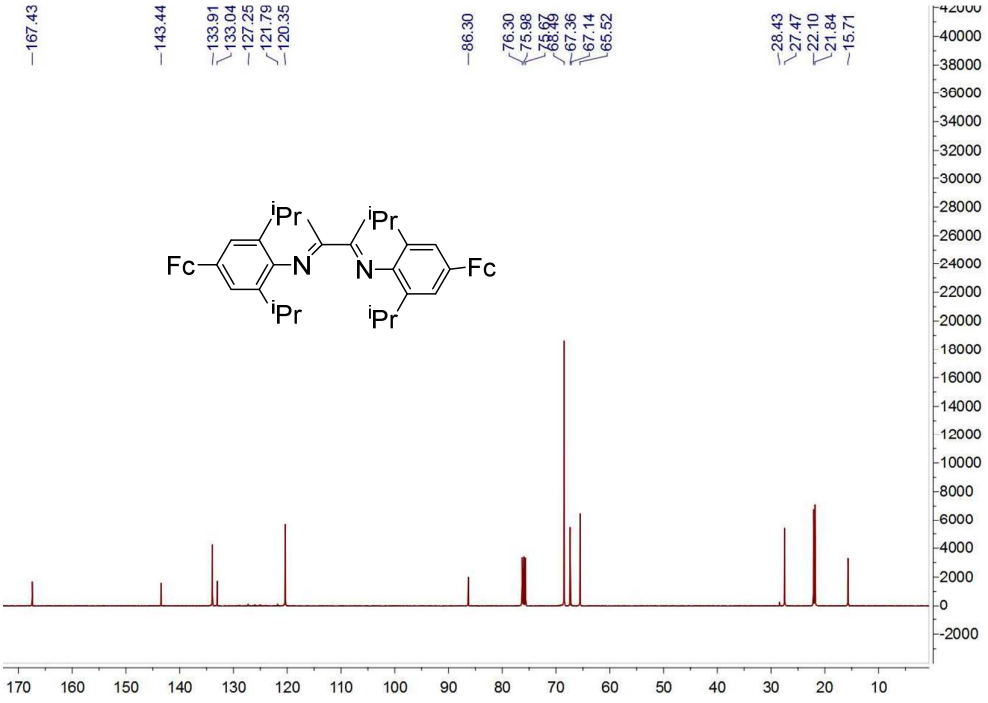

Figure S37. ^{13}C NMR spectrum of **L-Fc** in $CDCl_3$.

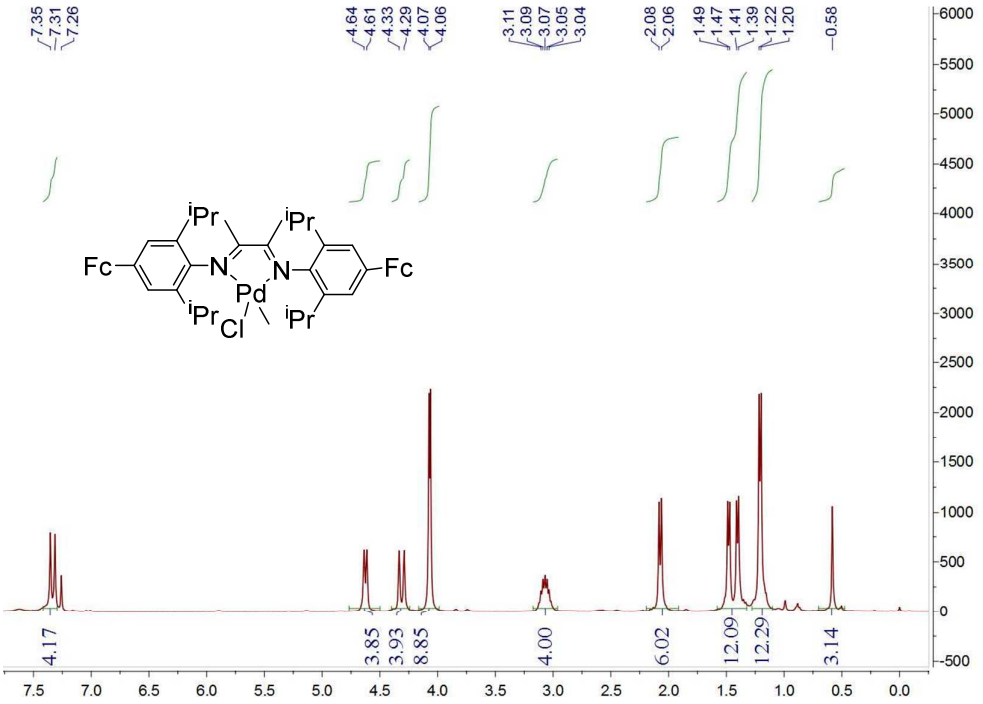

Figure S38. ^{1}H NMR spectrum of **Pd-Cl** in $CDCl_3$.

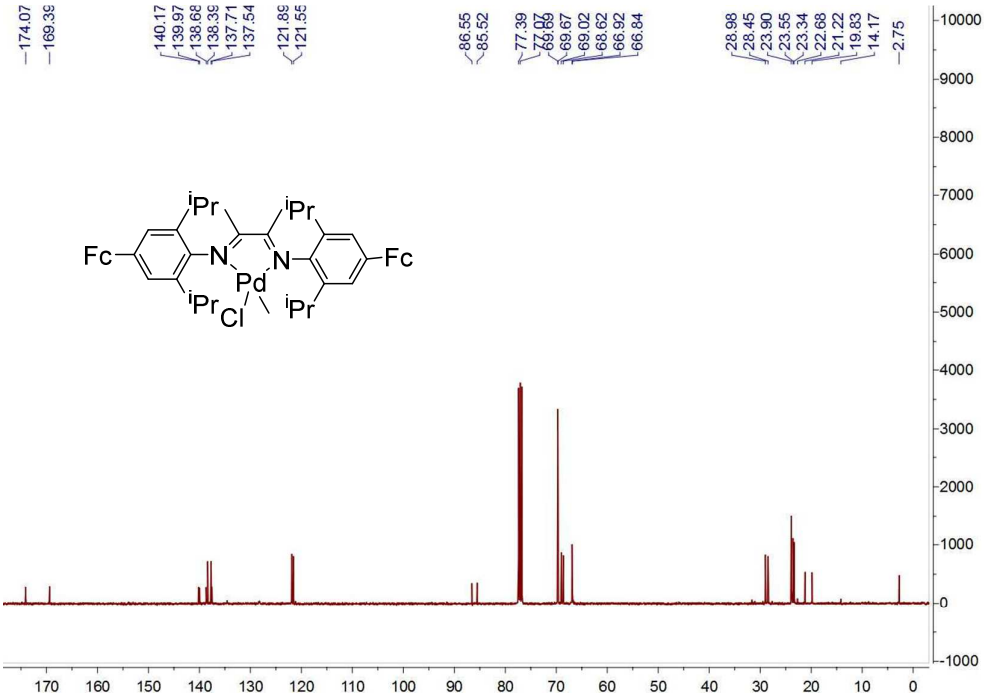

Figure S39. ^{13}C NMR spectrum of **Pd-Cl** in $CDCl_3$.

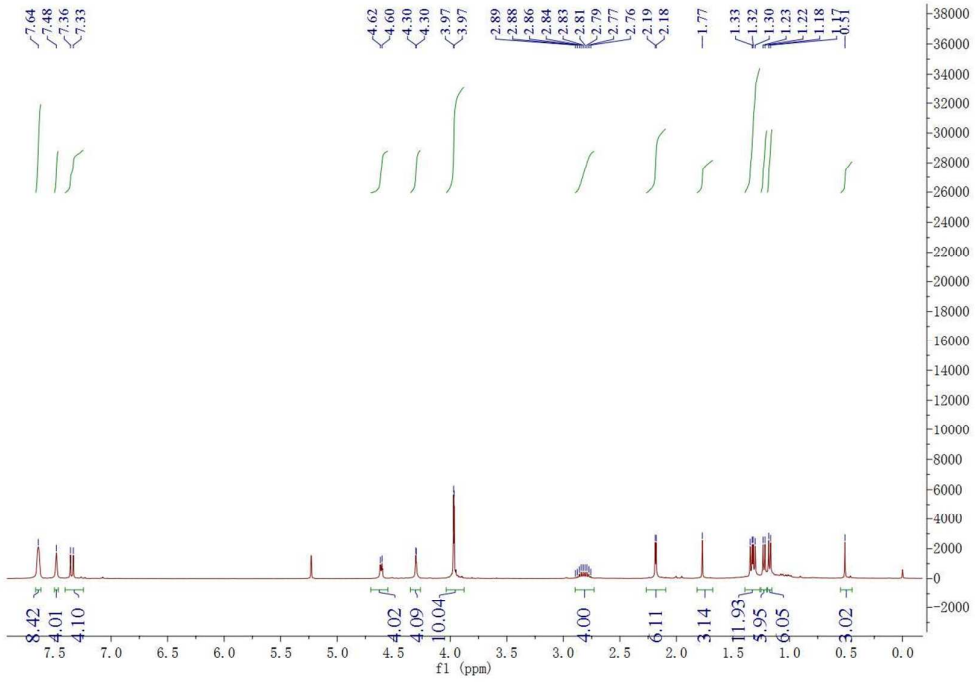

Figure S40. ^{1}H NMR spectrum of **Pd-CN** in CD_2Cl_2.

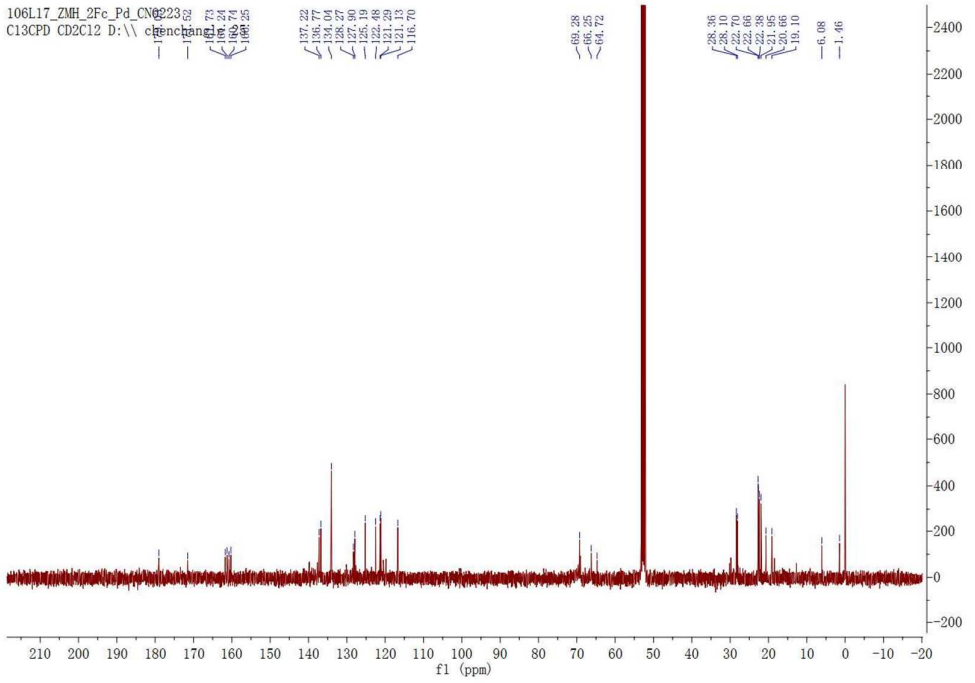

Figure S41. ^{13}C NMR spectrum of **Pd-CN** in CD_2Cl_2.

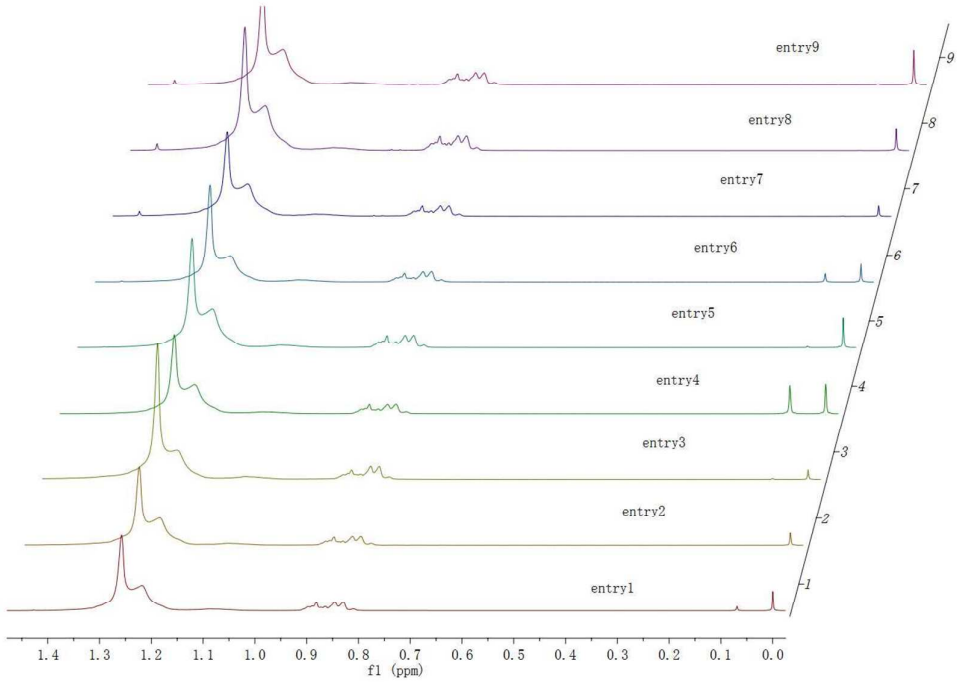

Figure S42. ^{1}H NMR spectrum of the polymer from table 1, entry 1-9 ($CDCl_3$, r.t.).

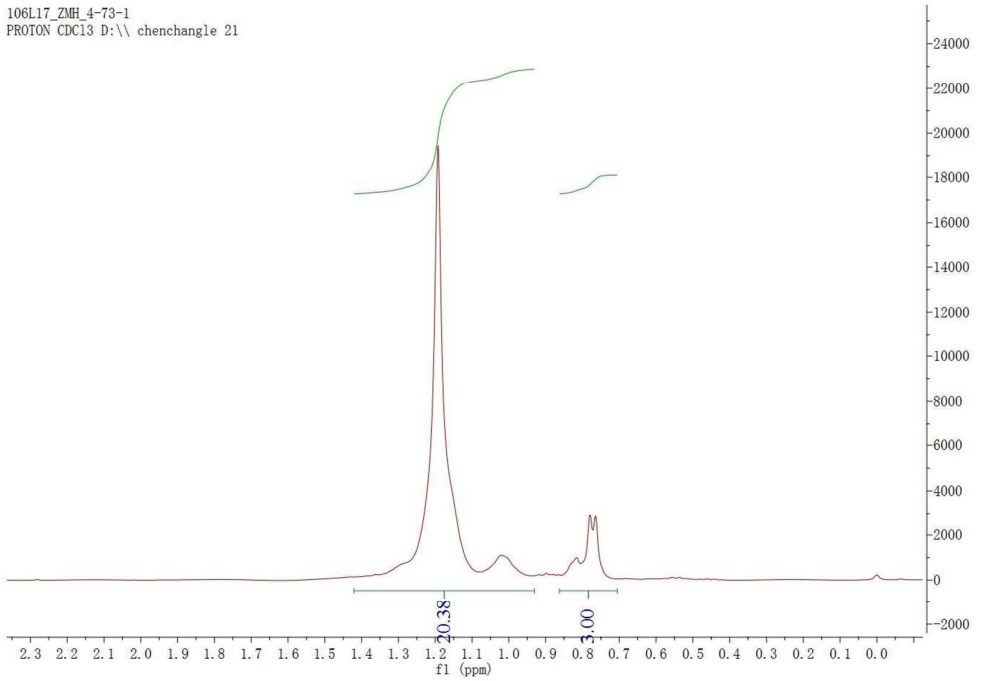

Figure S43. ^{1}H NMR spectrum of the polymer from table 1, entry 10 ($CDCl_3$, r.t.).

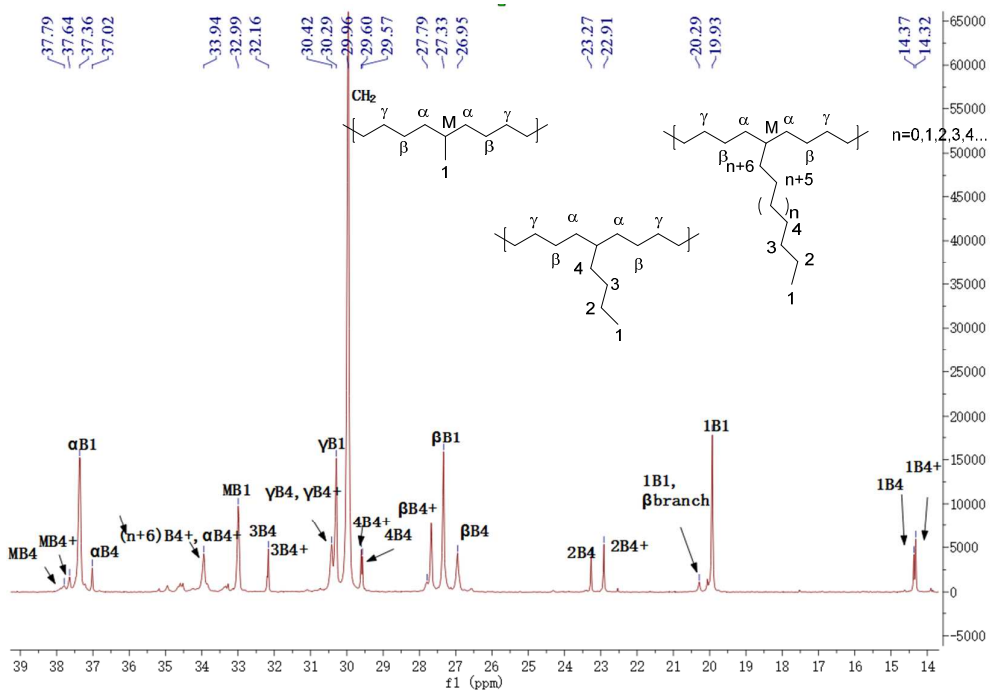

Figure S44. ^{13}C NMR spectrum of the polymer from table 1, entry 10 ($CDCl_3$, r.t.).

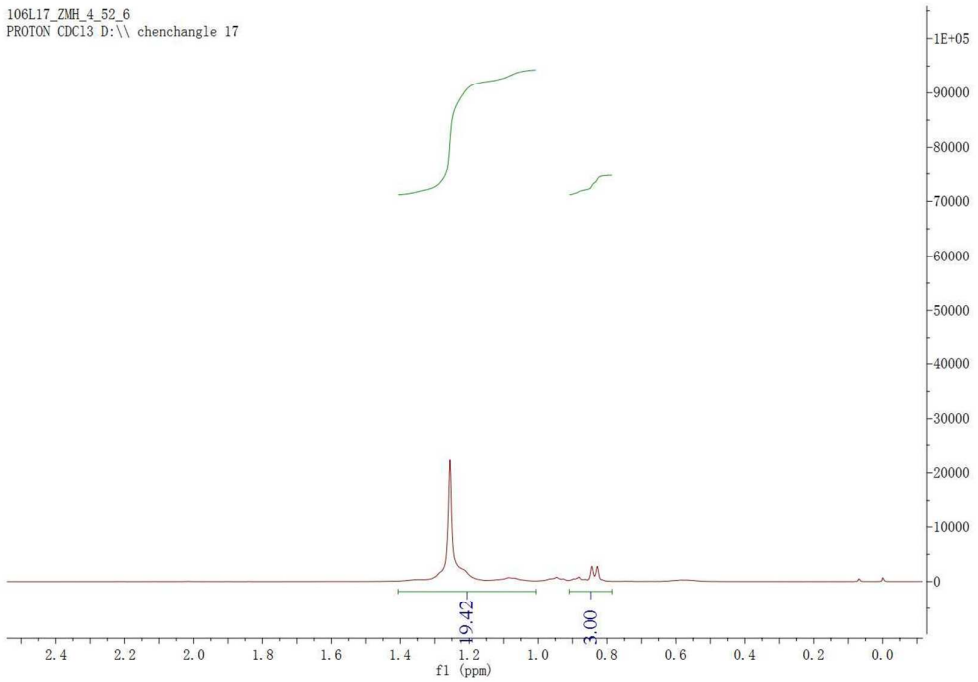

Figure S45. ^{1}H NMR spectrum of the polymer from table 1, entry 11 ($CDCl_3$, r.t.).

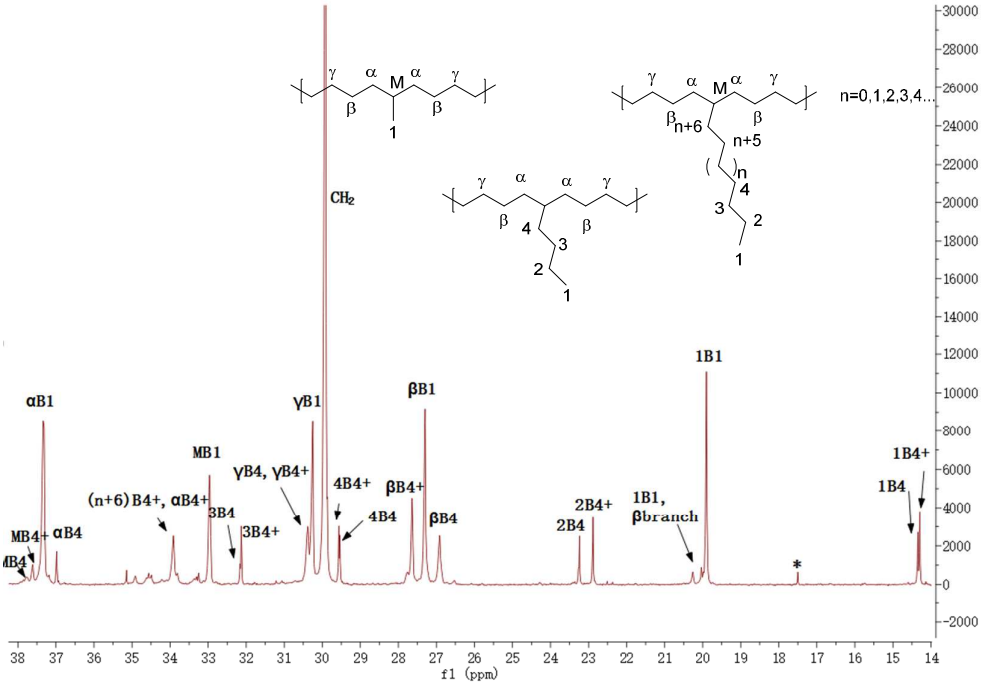

Figure S46. ^{13}C NMR spectrum of the polymer from table 1, entry 11 ($CDCl_3$, r.t.).

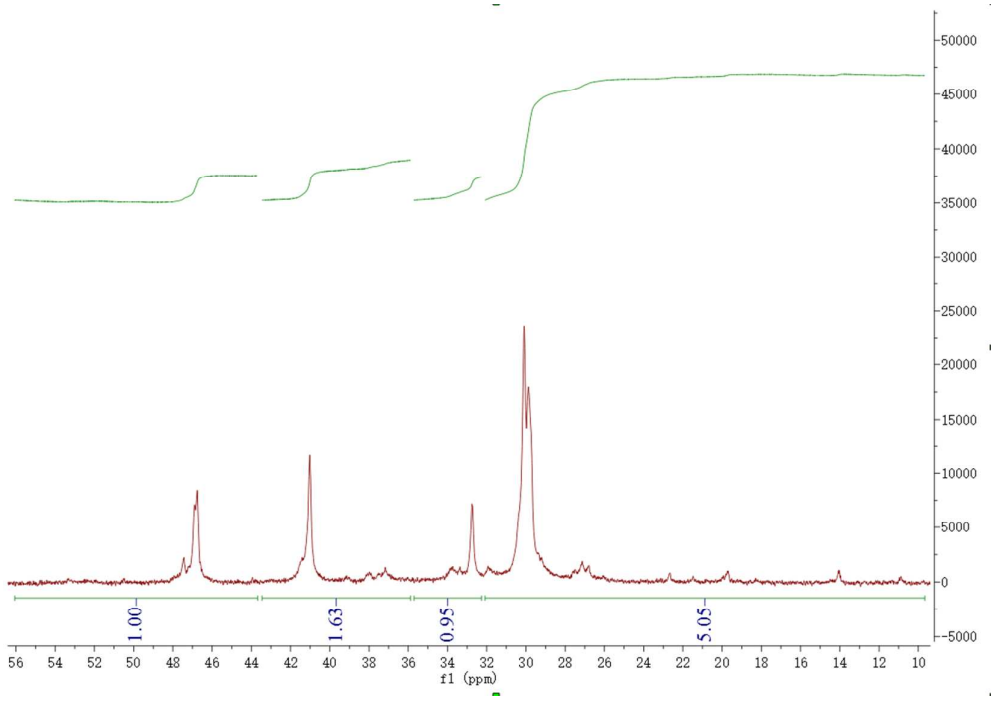

Figure S47. ^{13}C NMR spectrum of polyethylene-co-NB from table 2, entry 1 ($CDCl_3$, r.t.).

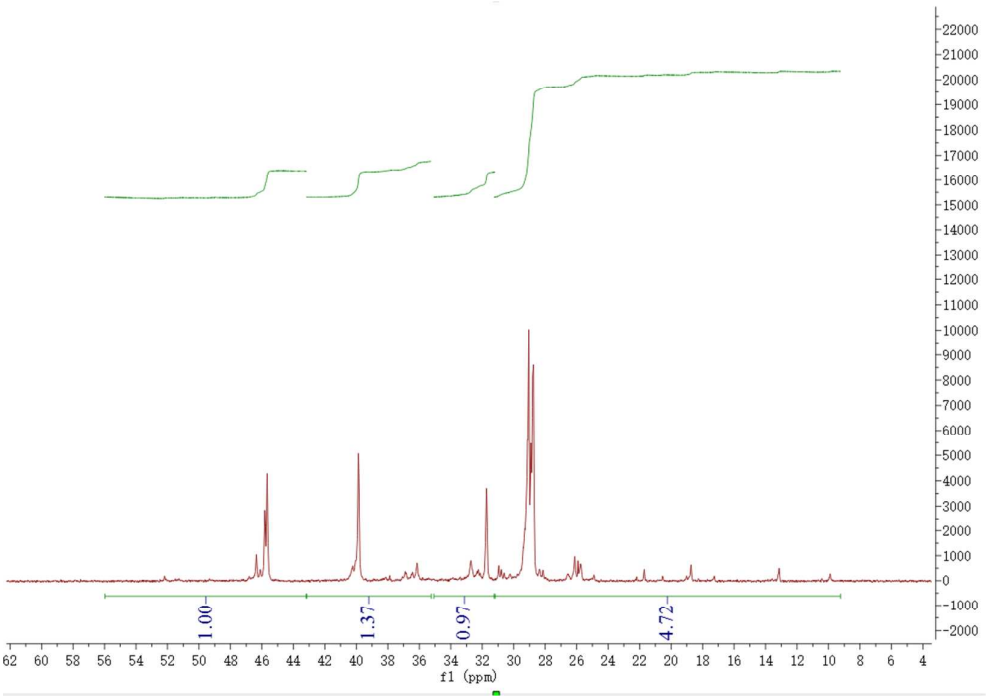

Figure S48 ^{13}C NMR spectrum of polyethylene-co-NB from table 2, entry 2 ($CDCl_3$, r.t.).

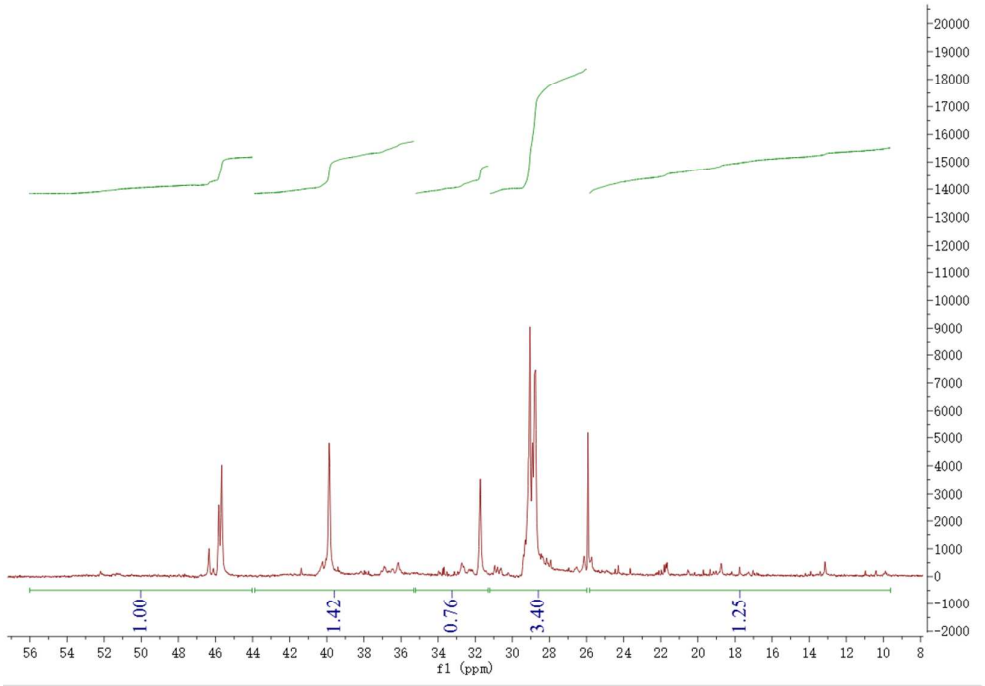

Figure S49. ^{13}C NMR spectrum of polyethylene-co-NB from table 2, entry 3 ($CDCl_3$, r.t.).

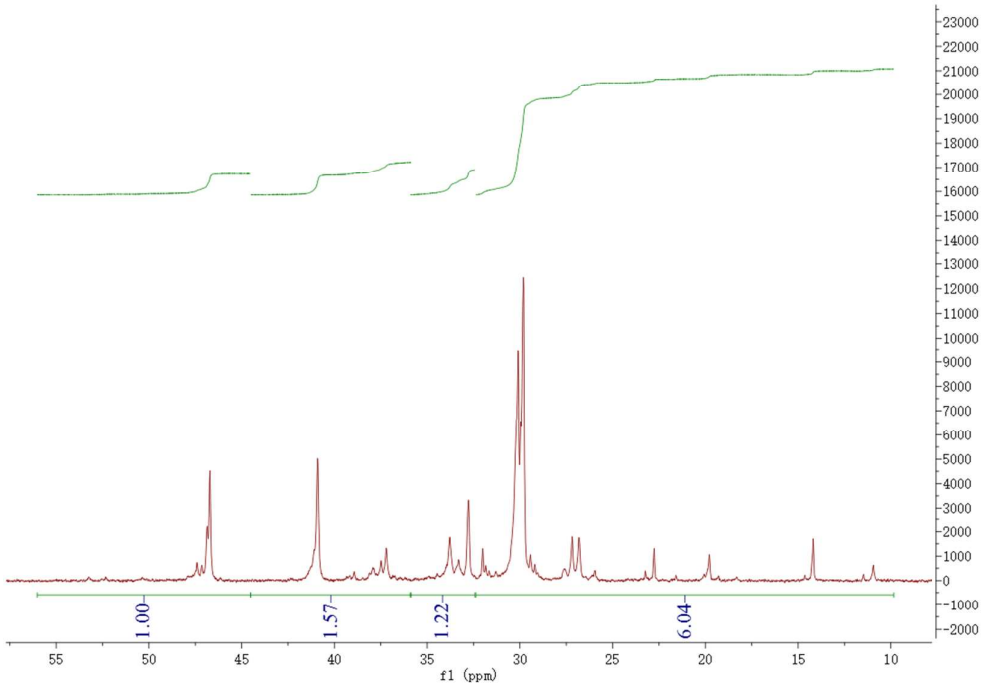

Figure S50. ^{13}C NMR spectrum of polyethylene-co-NB from table 2, entry 4 ($CDCl_3$, r.t.).

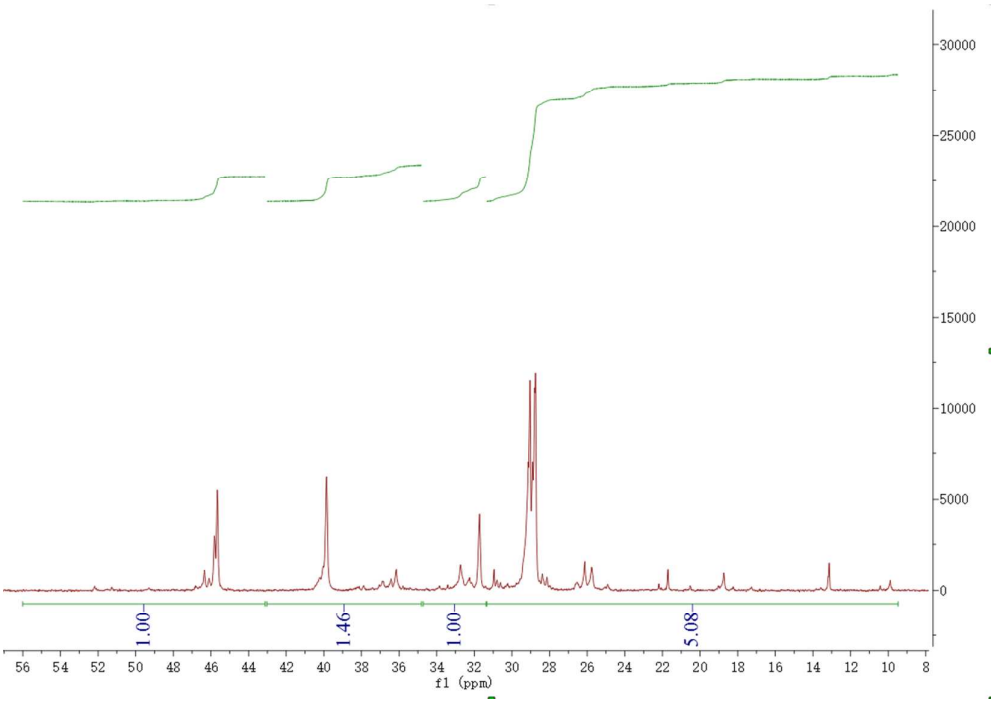

Figure S51. ^{13}C NMR spectrum of polyethylene-co-NB from table 2, entry 5 ($CDCl_3$, r.t.).

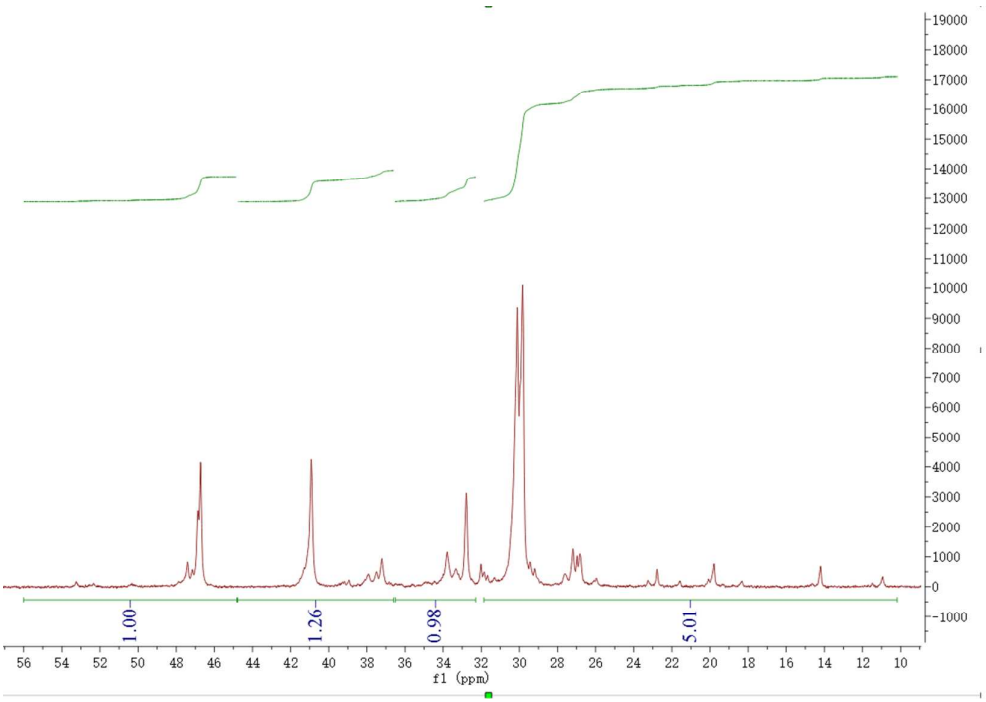

Figure S52. ^{13}C NMR spectrum of polyethylene-co-NB from table 2, entry 6 ($CDCl_3$, r.t.).

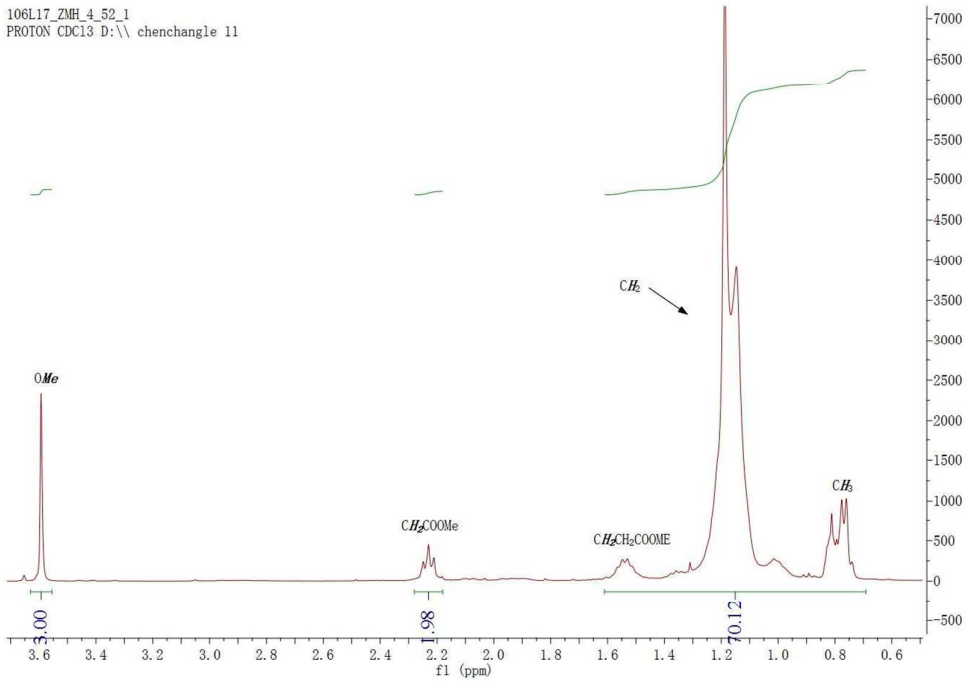

Figure S53. ^{1}H NMR spectrum of the polymer from table 2, entry 7 ($CDCl_3$, r.t.).

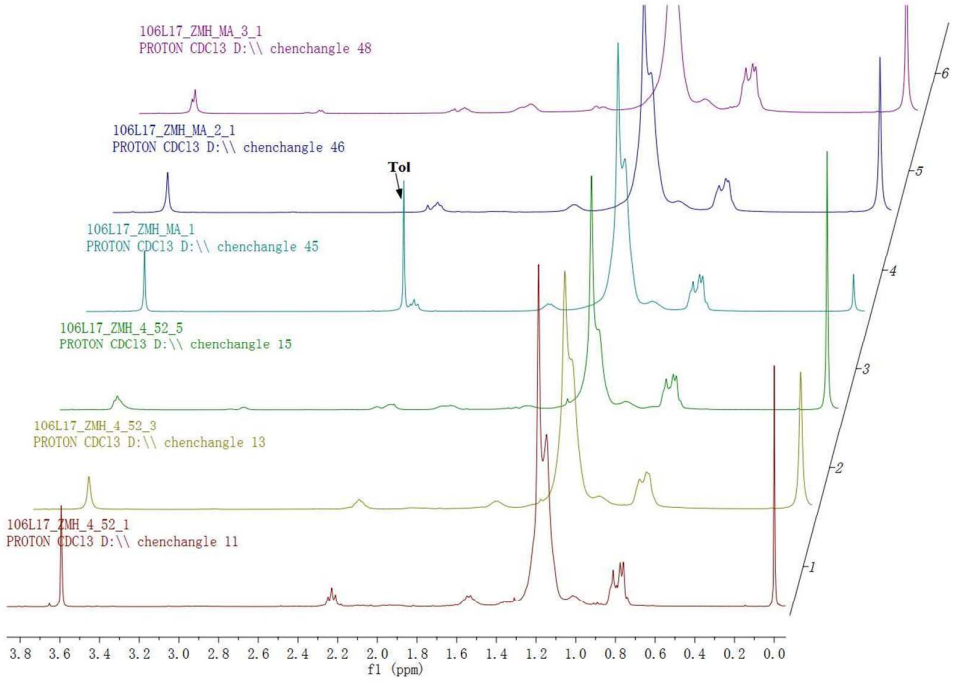

Figure S54. ^{1}H NMR spectrum of the polymer from table 2, from bottom to top entry 7-12 ($CDCl_3$, r.t.).

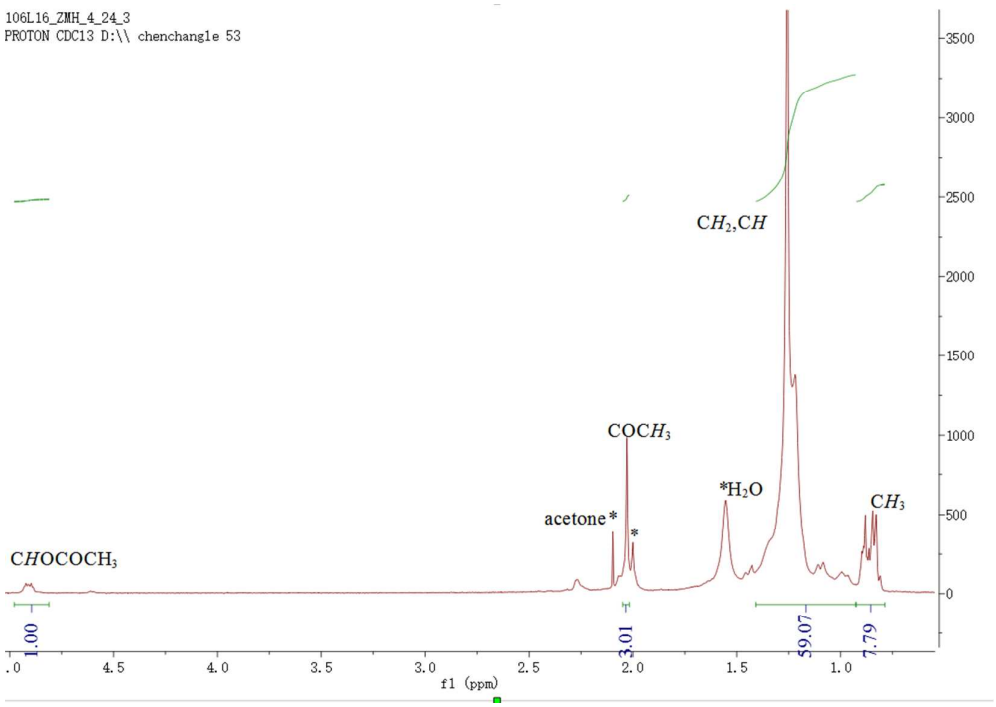

Figure S55. ^{1}H NMR spectrum of the polymer from table 2, entry 13 ($CDCl_3$, r.t.).

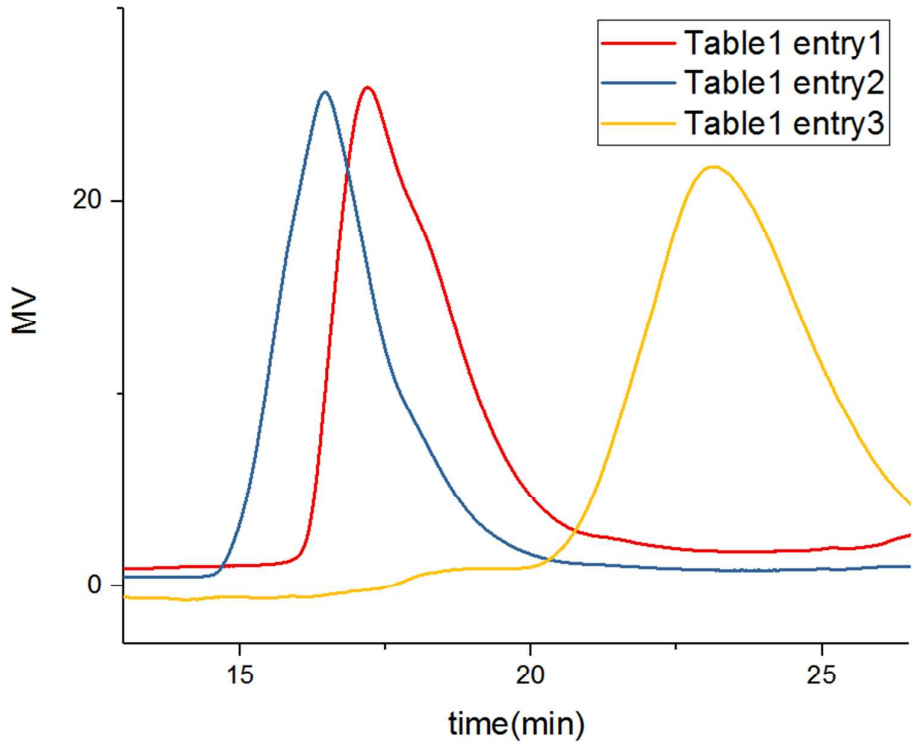

Figure S56. GPC trace of the polymer from table 1, entry 1-3.

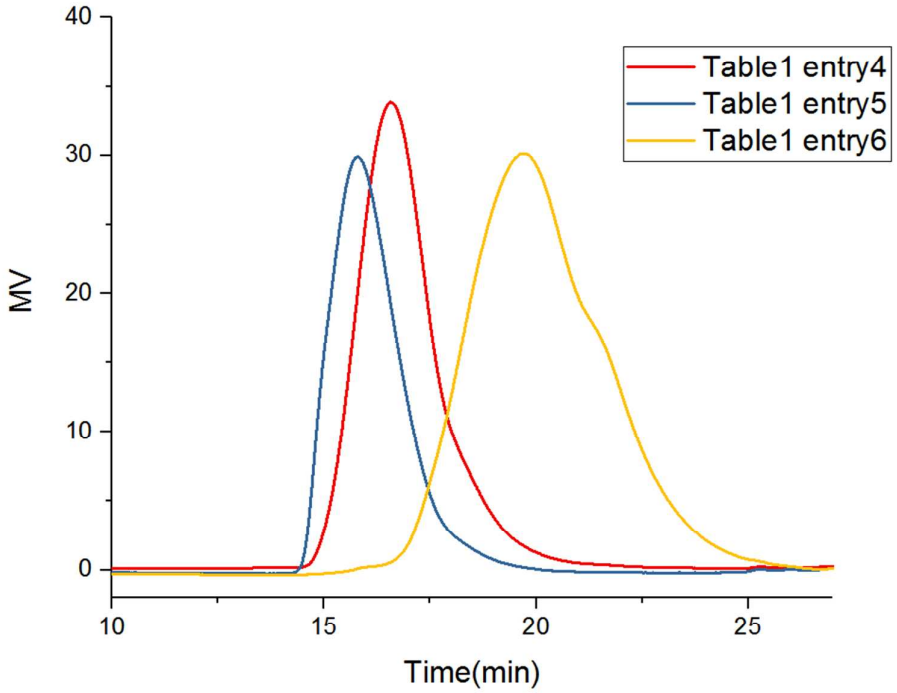

Figure S57. GPC trace of the polymer from table 1, entry 4-6.

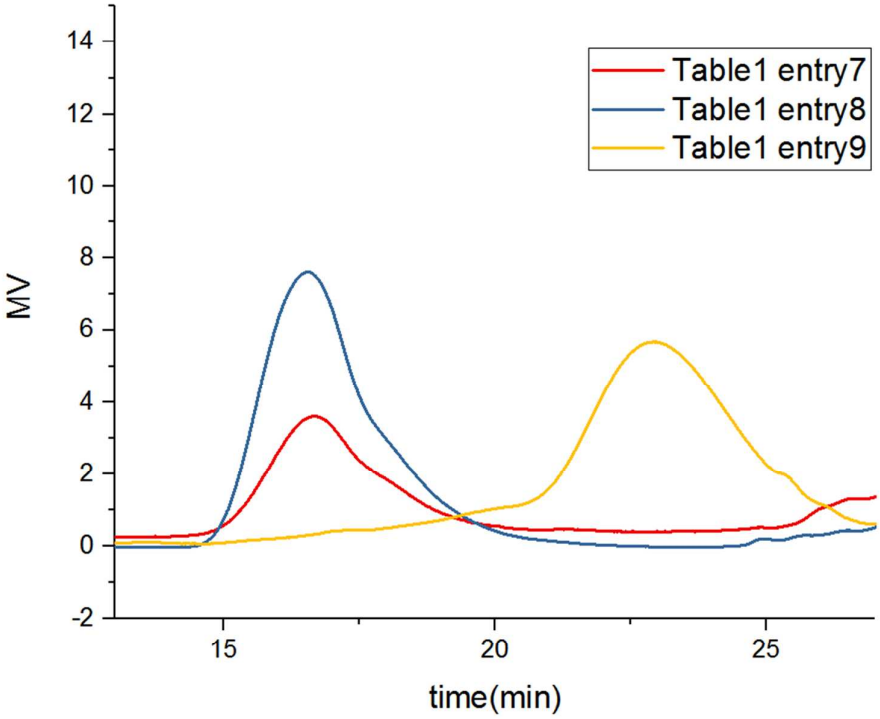

Figure S58. GPC trace of the polymer from table 1, entry 7-9.

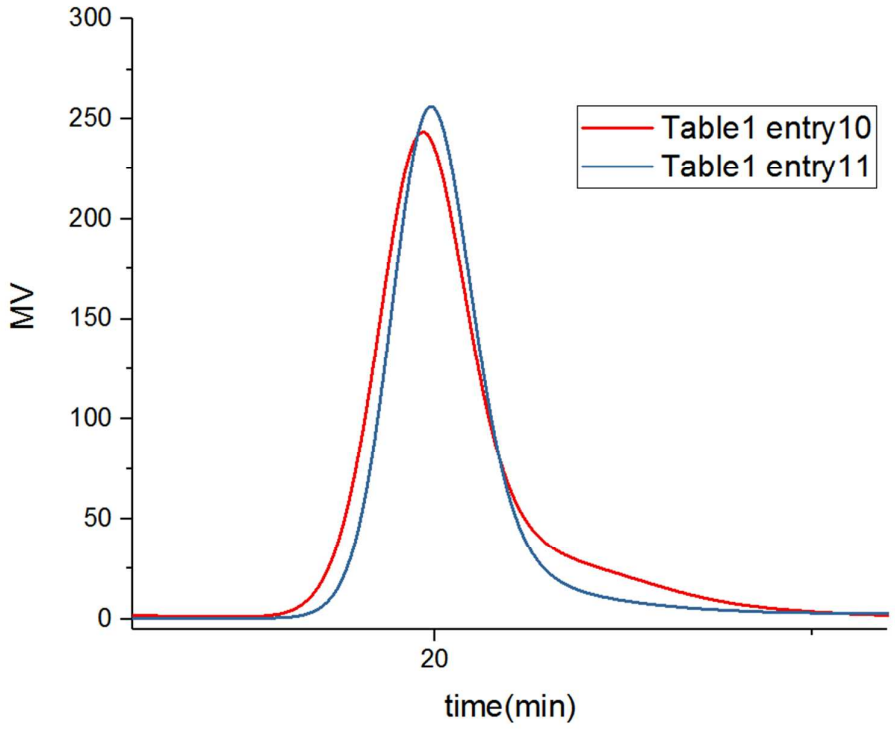

Figure S59. GPC trace of the polymer from table 1, entry 10-11.

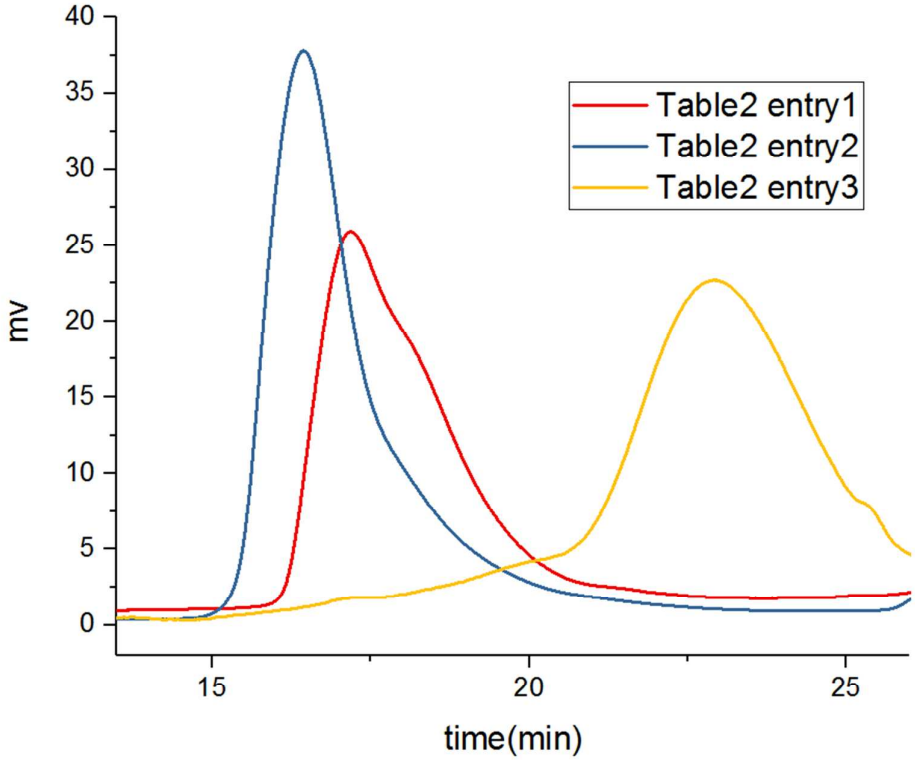

Figure S60. GPC trace of the polymer from table 2, entry 1-3.

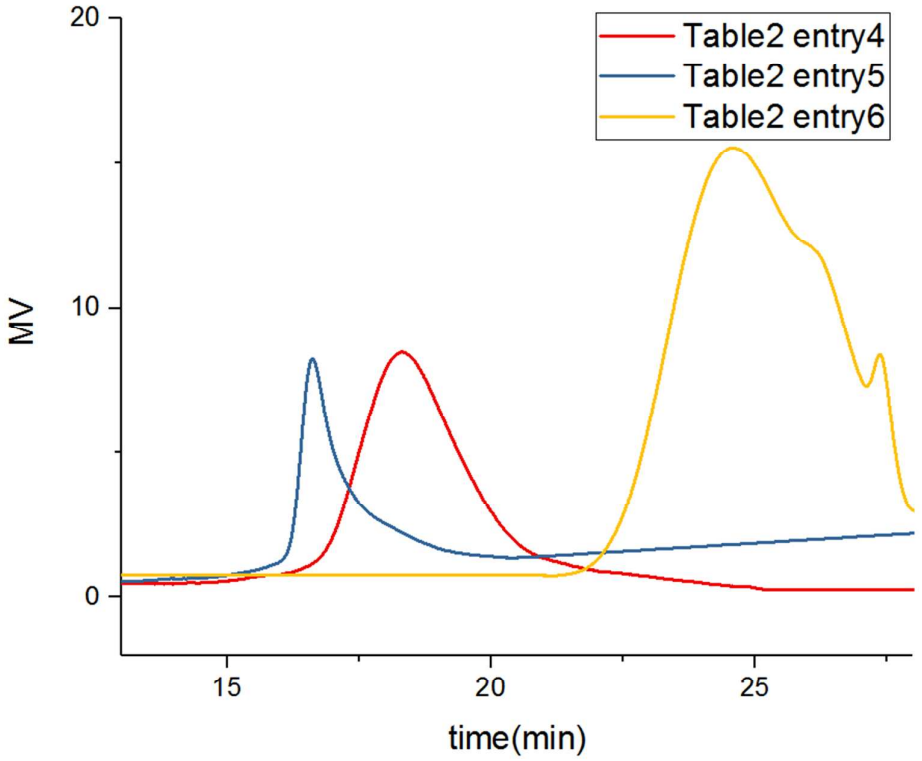

Figure S61. GPC trace of the polymer from table 2, entry 4-6.

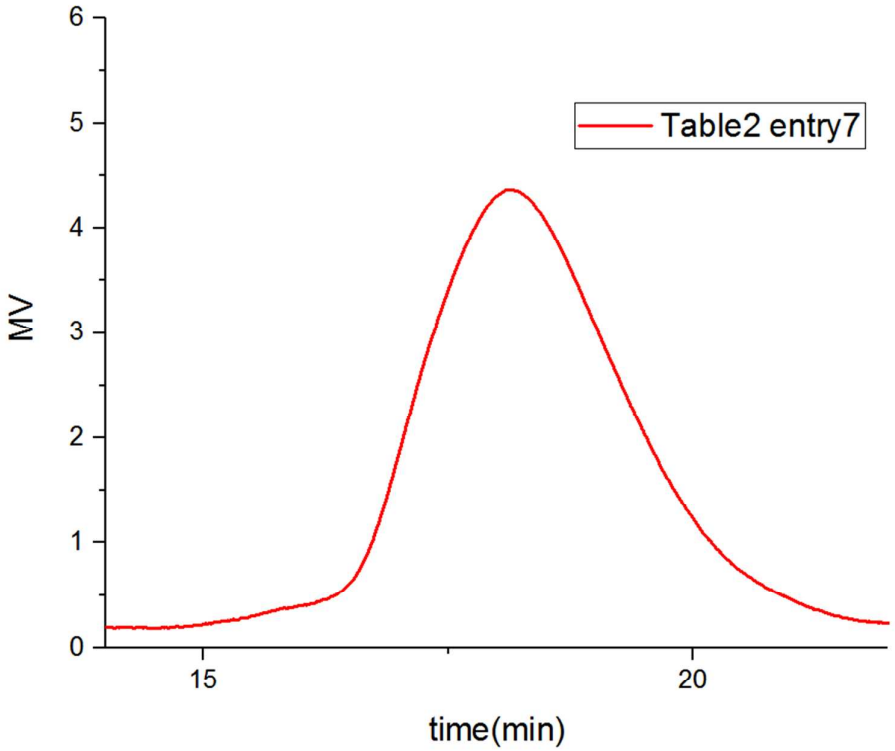

Figure S62. GPC trace of the polymer from table 2, entry 7.

3. References

(1) Siemeling, U.; Neumann, B.; Stammler, H, G.; Kuhnert, O. *Polyhedron* **1999,** 18, 1815-1819.

(2) Heintz, R, A.; Smith, J, A.; Szalay, P, S.; Weisgerber, A.; Dunbar, K, R.; *Inorganic Syntheses* **2002**, 33, 86-87.

(3) Kiesewetter, J.; Kaminsky, W. *Chem. Eur. J.* **2003**, 9, 1750-1758.

(4) Cotts, P, M.; Guan, Z, B.; MvCord, E.; McLain, S. *Macromolecules* **2000,** *33,* 6945-6952.

(5) (a) Zhong, H. A.; Labinger, J. A.; Bercaw, J. E. *J. Am. Chem. Soc.* **2002**, *124*, 1378-1399. (b) Popeney, C. S.; Guan, Z.; *Organometallics* **2005**, 24, 1145-1155.(c) Dai, S. Y.; Sui, X. L.; Chen, C. L. *Angew. Chem. Int. Ed.* **2015**, 54, 9948-9953.

4. X-ray Crystallography

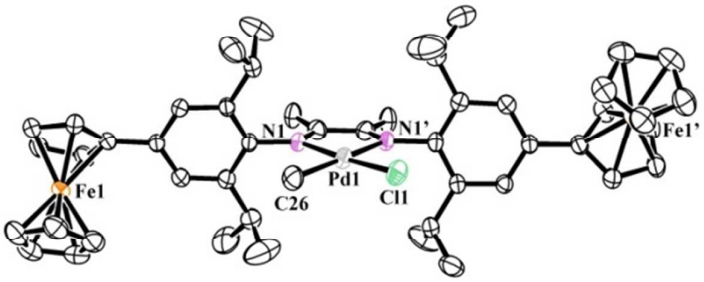

Figure S63. Molecular structures of **Pd-Cl**. Hydrogen atoms have been omitted for clarity. Selected bond lengths (Å) and angles (deg): Pd1−N1 2.102(4), Pd1−C26 2.04(3), Pd1−N1' 2.102(4), Pd1−Cl1 2.258(6), N1'−Pd1−C26 95.3(9), N1−Pd1−N1' 77.0(2), C26−Pd1−Cl1 87.2(8), N1'−Pd1−Cl1 100.6(2).

Table S3 Crystal data and structure refinement for Pd-Cl.

Entry	
Formula	C49 H59 Cl3 Fe2 N2 pd
Formula weight	1000.43
Temperature[K]	293(2)
λ(Mo-Kα)[Å]	1.54184
Crystal system	Monoclinic
Space group	C2/c
a[Å]	27.734(2)
b[Å]	9.9782(5)
c[Å]	18.5024(11)
α[°]	90.00
β[°]	18.5024(11)
γ[°]	90.00
Volume[$Å^3$]	4749.7(5)
Z	4
D(calc)[$g \cdot cm^{-3}$]	1.419
μ[mm^{-1}]	9.668
F(000)	2096
θ min-max (°)	4.7490-68.7250
h	-32→32
k	-11→7
l	-20→21
Reflections collected	9171
Reflections unique	4135
R(int)	0.0260
Data / restraints / parameters	4135 / 0 / 313
Final R indices [I>2σ(I)]	R_1 = 0.0454 wR_2 = 0.1162
R indices (all data)	R_1 = 0.0619 wR_2 = 0.1375
GOF on F^2	1.065